

Report No. UT-12.03

## HEALTH MONITORING OF PRECAST BRIDGE DECK PANELS REINFORCED WITH GLASS FIBER REINFORCED POLYMER (GFRP) BARS

### Prepared For:

Utah Department of Transportation  
Research Division

### Submitted By:

University of Utah  
Department of Civil & Environmental  
Engineering

### Authored By:

Chris P. Pantelides, Ph.D., S.E.  
Korin M. Holden, M.S.  
James Ries, M.S.

**March, 2012**

THIS PAGE LEFT INTENTIONALLY BLANK

## **DISCLAIMER**

“The authors alone are responsible for the preparation and accuracy of the information, data, analysis, discussions, recommendations, and conclusions presented herein. The contents do not necessarily reflect the views, opinions, endorsements, or policies of the Utah Department of Transportation and the US Department of Transportation. The Utah Department of Transportation makes no representation or warranty of any kind, and assumes no liability therefore.”

THIS PAGE LEFT INTENTIONALLY BLANK

## UDOT RESEARCH & DEVELOPMENT REPORT ABSTRACT

1 Report No. <p style="text-align: center;">UT-12.03</p>	2. Government Accession No.	3. Recipient's Catalog No.	
4. Title and Subtitle <b>HEALTH MONITORING OF PRECAST BRIDGE DECK PANELS REINFORCED WITH GLASS FIBER REINFORCED POLYMER BARS.</b>		5. Report Date <p style="text-align: center;">March, 2012</p>	
		6. Performing Organization Code <p style="text-align: center;">17361G</p>	
7. Author <p style="text-align: center;">Chris P. Pantelides, Korin M. Holden, James Ries</p>		8. Performing Organization Report No. <p style="text-align: center;">53500088</p>	
9. Performing Organization Name and Address University of Utah Department of Civil and Environmental Engineering 110 S. Central Campus Dr., Room 2115 Salt Lake City, Utah 84112		10. Work Unit No. <p style="text-align: center;">AM09.002</p>	
		11. Contract or Grant No. <p style="text-align: center;">10-9012</p>	
12. Sponsoring Agency Name and Address Utah Department of Transportation 4501 South 2700 West Salt Lake City, Utah 84114-8410		13. Type of Report & Period Covered <p style="text-align: center;">FINAL</p>	
		14. Sponsoring Agency Code <p style="text-align: center;">8RD1251H</p>	
16. Abstract <p>The present research project investigates monitoring concrete precast panels for bridge decks that are reinforced with Glass Fiber Reinforced Polymer (GFRP) bars. Due to the lack of long term research on concrete members reinforced with GFRP bars, long term health monitoring is important to record the performance and limit states of the GFRP decks and bridge as a whole. In this research, data is collected on concrete strains, bridge deflections, vertical girder accelerations, as well as initial truck load testing and lifting strains.</p>			
17. Key Words GFRP bars; bridge deck; long term health monitoring; strains; vertical accelerations; deflections		18. Distribution Statement UDOT Research Division 4501 South 2700 West Salt Lake City Utah 84114-8410	
23. Registrant's Seal			
19. Security Classification (of this report) <p style="text-align: center;">Unclassified</p>	20. Security Classification (of this page) <p style="text-align: center;">Unclassified</p>	21. No. of Pages <p style="text-align: center;">105</p>	22. Price

THIS PAGE LEFT INTENTIONALLY BLANK

## **ACKNOWLEDGEMENTS**

The research reported in this report was supported by the Utah Department of Transportation (UDOT). The authors acknowledge the contributions of Campbell Scientific, Hughes Bros Inc., and the assistance of Professor Lawrence D. Reaveley, Mark Bryant, Brandon T. Besser, and Clayton A. Burningham, Erika D. Weber, Ruifen Liu, Shannon Hansen, Shawn H. Malan, Zac Jones and Wade Stinson of the University of Utah in the experimental portion of the research. The authors also acknowledge the contributions of the UDOT Technical Advisory Committee (TAC): Ms. Carmen Swanwick, Ms. Rebecca Nix, Mr. Daniel Hsiao, and Mr. Abdul Wakil. Special thanks to Rebecca Nix at UDOT for providing the research opportunity, information and support.

THIS PAGE LEFT INTENTIONALLY BLANK

## TABLE OF CONTENTS

DISCLAIMER .....	ii
<b>UDOT RESEARCH &amp; DEVELOPMENT REPORT ABSTRACT.....</b>	<b>iv</b>
<b>ACKNOWLEDGEMENTS .....</b>	<b>vi</b>
<b>EXECUTIVE SUMMARY.....</b>	<b>xvi</b>
<b>1.0 INTRODUCTION.....</b>	<b>1</b>
1.1 Overview of Glass Fiber Reinforced Polymers Bars .....	6
1.2 Material Properties of GFRP Bars .....	9
1.3 Design of Bridge And Changes In Design To Accommodate GFRP Reinforcement	10
<b>2.0 EXPERIMENTAL DESIGN.....</b>	<b>13</b>
2.1 Experimental Setup .....	14
2.2 Instrumentation Setup .....	19
2.2.1 Electrical Strain Gauges .....	20
2.2.2 Vibrating Wire Strain Gauges .....	21
2.2.3 Linear Variable Differential Transducer (LVDT).....	23
2.2.4 Accelerometers.....	23
2.2.5 Atmospheric .....	24
2.2.6 Surveying Equipment.....	24
2.2.7 Camera .....	25
2.3 Data Acquisition And Remote Data Transfer .....	27
<b>3.0 EXPERIMENTAL OBSERVATIONS .....</b>	<b>35</b>
3.1 Experimental Observations For Lifting And Transport .....	35
3.1.1 First Lift.....	35
3.1.2 Second Lift .....	36

3.1.3 Transport .....	37
3.1.4 Third Lift .....	38
3.2 Post Tensioning Observations .....	39
3.3 Truck Load Test Observations .....	41
3.3.1 Vibrating Wire Strain Gauges .....	41
3.3.2 Linear Variable Displacement Transducers .....	43
3.3.3 Girder Deflections .....	46
3.3.4 Accelerometers .....	48
<b>4.0 ANALYTICAL RESULTS .....</b>	<b>59</b>
4.1 Lifting Curvature Diagram .....	59
4.2 Post Tensioning .....	60
4.3 Panel Deflections .....	61
4.4 Girder Deflections .....	61
4.5 Accelerometers .....	62
4.6 Modeling .....	64
4.6.1 Bridge Finite Element .....	64
4.6.2 Deck Panel Lifting Strains .....	70
4.7 Cost Analysis .....	77
<b>5.0 CONCLUSIONS .....</b>	<b>81</b>
<b>6.0 REFERENCES .....</b>	<b>85</b>

## TABLE OF FIGURES

Figure	Page
1. Location of Bridge on US-6.....	2
2. Plan of Bridge .....	3
3. Bridge cross-section looking east .....	3
4. Bridge plan showing panels and girders .....	4
5. Panel EP3 sitting in the precast yard with approach slab rebar to the right.....	4
6. Leveling bolts and shear stud blockouts .....	5
7. Close-up of GFRP bar.....	6
8. Steel reinforcement to accommodate increased shear demand from post-tensioning anchor .....	11
9. Panel P2-05 being lifted using straps at the bridge site .....	15
10. Lifting point diagram (all dimensions in inches).....	15
11. Test truck dimensions .....	17
12. Locations of trucks during truck load test.....	18
13. Plan of bridge with instruments and panel.....	20
14. Electrical gauge locations for both panels .....	21
15. Vibrating Wire Strain Gauge locations.....	22
16. Close up of Vibrating Wire Strain Gauge attached to GFRP rebar .....	22
17. Linear Variable Displacement Transducer attached to diaphragm under bridge .....	23
18. HMP-50 in its protective housing attached to fence post adjacent to bridge.....	24
19. Surveying team for truck load test .....	25
20. Still camera used for visual record of truck causing large accelerations .....	26
21. Instrument locations on the bridge.....	26
22. Location of camera with respect to bridge.....	27
23. Equipment setup for initial lifting.....	31
24. Equipment setup for transportation, 2nd and 3rd lifting.....	32
25. Equipment setup for truck load test .....	33

26. Equipment setup for long term monitoring.....	34
27. Strain profile for P2-05 during its first lift removing it from the formwork.....	35
28. Strain profile for panel EP3 during its second lift .....	36
29. Max, min, and average in all gauges during lifting and transport of panel EP3.....	37
30. Strain profile for EP3 during its third lift.....	38
31. Post tensioning strains in bridge deck.....	40
32. Locations of VWSGs for measuring strains due to post-tensioning.....	40
33. Two-year concrete strain record .....	42
34. Deck deflections from testing for Truck A, Sept. 29, 2009 .....	43
35. Deck deflections from testing for Truck B, Sept. 29, 2009 .....	44
36. Deck deflections from testing for Truck A and Truck B; Sept. 29, 2009.....	44
37. Deck deflections from testing for Truck A and Truck B; Sept. 1, 2010 .....	45
38. Midspan girder deflections for tests 7 through 9 for Girder #4 .....	47
39. Girder deflections for truck load test 9 .....	48
40. Acceleration record for Truck B traveling at 40 mph for Test 1. ....	49
41. Maximum accelerations for Truck B traveling at 40 mph.....	49
42. Maximum accelerations for Truck B traveling at 65 mph.....	50
43. Maximum accelerations from second truck load test performed Sept. 1, 2010, as a function of truck speed .....	50
44. Maximum accelerations from third truck load test performed Nov. 19, 2010, as a function of truck speed .....	51
45 Acceleration record of Oct. 22, 2010 during a construction period.....	52
46. Image for acceleration record of Oct. 22, 2010 during a construction period. ....	52
47. Acceleration of 0.075 g at girder 2 on October 31, 2011 .....	53
48. Acceleration of 0.078 g at girder 2 on November 1, 2011 .....	54
49. Acceleration of 0.074 g at girder 2 on November 2, 2011 .....	54
50. Sample of trucks in the data set and their corresponding acceleration response .....	56
51. Acceleration as a function of weight and speed from Nov. 21, 2011 test .....	57
52. Curvature diagram from experimental results (arrows represent lifting points).....	59
53. Acceleration data from first truck load test, September 2009 .....	62
54. Dynamic Deflection of 43 kip truck at 65 mph over girder 4.....	63

55. Model showing lanes, girders and abutments .....	65
56. Finite Element model of the dead loads; maximum deflection is -0.201 inches .....	66
57. Finite Element model of the prestress loads; maximum deflection is +0.0003 inches.....	66
58. Finite Element model of the truck loads at midspan in the inside lane; maximum deflection is -0.003 inches .....	67
59. Total bridge deflection of -0.203 inches under AASHTO LRFD Service I load case combination.....	67
60. Mode 1, period of 0.146 s .....	68
61. Mode 2, period of 0.146 s .....	68
62. Stress on bridge deck with a maximum of 913 psi and a minimum of -393 psi.....	69
63. Static truck load at midspan in inside lane; deflection of -0.003 inches.....	69
64. Deflected panel with a maximum deflection of 0.002 inches.....	71
65. Midline deflection for panel sitting on the ground .....	71
66. Maximum stress of 96 psi in the panel and 160 psi at supports .....	72
67. Mid-line strains in panel while on ground .....	72
68. Maximum stress of 100 psi at the top of deck panel while lifting .....	73
69. Mid-line strain without parapet.....	74
70. Deflected panel with a maximum midline deflection of 0.026 in.....	74
71. Mid-line deflection for panel lifting without the parapet.....	75
72. Deflected panel with a maximum midline deflection of 0.34 in.....	75
73. Midline deflection for panel lifting with the parapet .....	76
74. Stress of panel with parapet while lifting is 276 psi max .....	76
75. Mid-line strain with parapet.....	77

THIS PAGE LEFT INTENTIONALLY BLANK

## LIST OF TABLES

1. Material properties of GFRP bars used at the Beaver Creek Bridge .....	8
2. Comparison between Aslan 100 GFRP & Grade 60 Steel .....	9
3. Truck Weights.....	16
4. Static Tests .....	17
5. Initial Dynamic Test Details at Bridge Opening.....	19
6. Deck deflections relative to girders (inches) .....	46
7. Comparison of collected data to computer generated model.....	70
8. Cost analysis Deck Cost Analysis for Beaver Creek Bridge .....	79

THIS PAGE LEFT INTENTIONALLY BLANK

## **EXECUTIVE SUMMARY**

The Beaver Creek Bridge on US-6 is a pilot project for Glass Fiber Reinforced Polymer (GFRP) reinforced precast post-tensioned bridge decks in the State of Utah. The bridge was built in 2009, using precast prestressed girders, as well as precast deck panels. The west-bound bridge decking was composed of 12 precast panels each measuring 41'-5" long, 6'-10" wide, and 9¼" thick, and weighing approximately 33 kips. At the time, these panels were the longest GFRP reinforced panels in the United States. The Utah Department of Transportation has decided to evaluate GFRP reinforcing bars as an alternative to steel rebar in this bridge deck. The hope is to increase the lifespan of bridge decks to match the service life of the entire bridge. Due to the nature of GFRP bars, the panels were lifted at 4 points using straps instead of embedded anchors. During 4-point lifting, the panels exhibited small deflections and strains. Furthermore, no cracks larger than hairline cracks were found in the panels after lifting.

The Beaver Creek bridge deck is the first precast deck in the State of Utah to be post-tensioned in the direction of traffic. Post-tensioning bridge decks is expected to become standard procedure in the State of Utah. Post-tensioning of the panels results in increased continuity between panels and protection of the joints from potential corrosion. Long term monitoring of 2 precast deck panels and other structural elements of the bridge are detailed in this report to UDOT. Details of the bridge deck utilizing the precast concrete panels are provided. The performance of the supporting prestressed girders during 4 truck load tests, carried out at various times, is examined and a performance evaluation is made herein. Static and dynamic truck load test results are discussed and conclusions are made regarding the response observed from the bridge deck deflections, and girder impact factors. From continuous monitoring, loads applied to

the bridge are remotely collected and the data analyzed. The collected data includes strains and curvature of the deck panels, relative displacements of the panels with respect to the girders and vertical accelerations of the girders measured through accelerometers from loads applied to the deck, based on the weight and speed of the truck. Using the curvature, displacement and acceleration data, conclusions are made regarding the response of the deck by comparing test results to design requirements. Results are compared as well to a finite element analyses from computer generated models.

The use of GFRP bars has the potential to extend the life of bridge decks exposed to deicing salts from 45years to 100-years, while only requiring an increased capital cost in the bridge of approximately 8%. Furthermore, the use of GFRP bars in conjunction with accelerated construction practices has the potential to reduce long term user delays resulting from maintenance. The difference in capital cost could decrease as designers become more comfortable with GFRP bars and gain experience with the system. Based on monitoring of the precast concrete bridge deck panels reinforced with GFRP bars, it is shown that after 2 years in service, the performance of the bridge including the precast deck is well within the design requirements.

## **1.0 INTRODUCTION**

In recent years, the Utah Department of Transportation (UDOT) has taken progressive measures to increase the lifespan of its bridges as well as to decrease user delays. These measures include the use of accelerated bridge construction practices and the exploration of materials which decrease scheduled maintenance resulting from corrosion. UDOT decided to evaluate Glass Fiber Reinforced Polymer (GFRP) reinforcing bars as an alternative to steel rebar in bridge decks. The evaluation is to determine if its use would increase the lifespan of bridge decks to match the service life of the entire bridge.

During the summer of 2009, construction began on the Beaver Creek Bridge, located approximately 20 miles north of Price, Utah on US-6, as seen in Figure 1. The Beaver Creek Bridge deck was constructed using precast panels reinforced with GFRP bars instead of traditional steel reinforcing bars. GFRP bars offer many advantages over traditional steel reinforcing bars, including increased tensile strength, decreased unit weight and corrosion resistance. Using GFRP bars in a bridge deck has been hypothesized to extend the life of the bridge deck up to 100 years (Benmokrane et al. 2006).

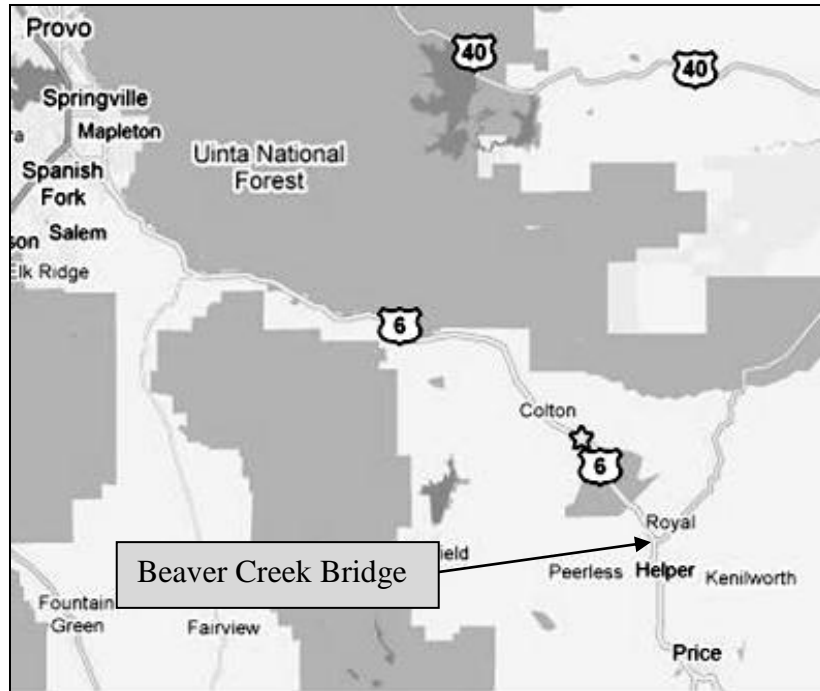


**Figure 1. Location of Bridge on US-6**

The Beaver Creek Bridge is a single span creek crossing with access for wildlife passage. The bridge is composed of 12 AASHTO Type IV prestressed girders (AASHTO 2009) running the span of the bridge with precast concrete panels lying perpendicular to the girders, 12 panels for each direction of traffic. The bridge has an overall span length of 88'-2" and an out-to-out width of 88'-10", as shown in Figure 2. The deck was designed per American Concrete Institute (ACI) 440.1 R-06 (2006), and constructed using 24 precast deck panels reinforced with GFRP bars. The bridge was constructed in 2 phases, 1 for each direction of traffic. In Phase I, the east-bound direction was constructed, and was composed of 12 precast panels measuring 44'-5" long, 6'-10" wide, and 9¼" thick. In Phase II, the west-bound bridge was constructed, its deck was composed of 12 panels each measuring 41'-5" long, 6'-10" wide, and 9¼" thick, and weighing

approximately 33 thousand pounds (kips), as seen in Figures 3-5. The project focuses on Phase II of the Beaver Creek Bridge.

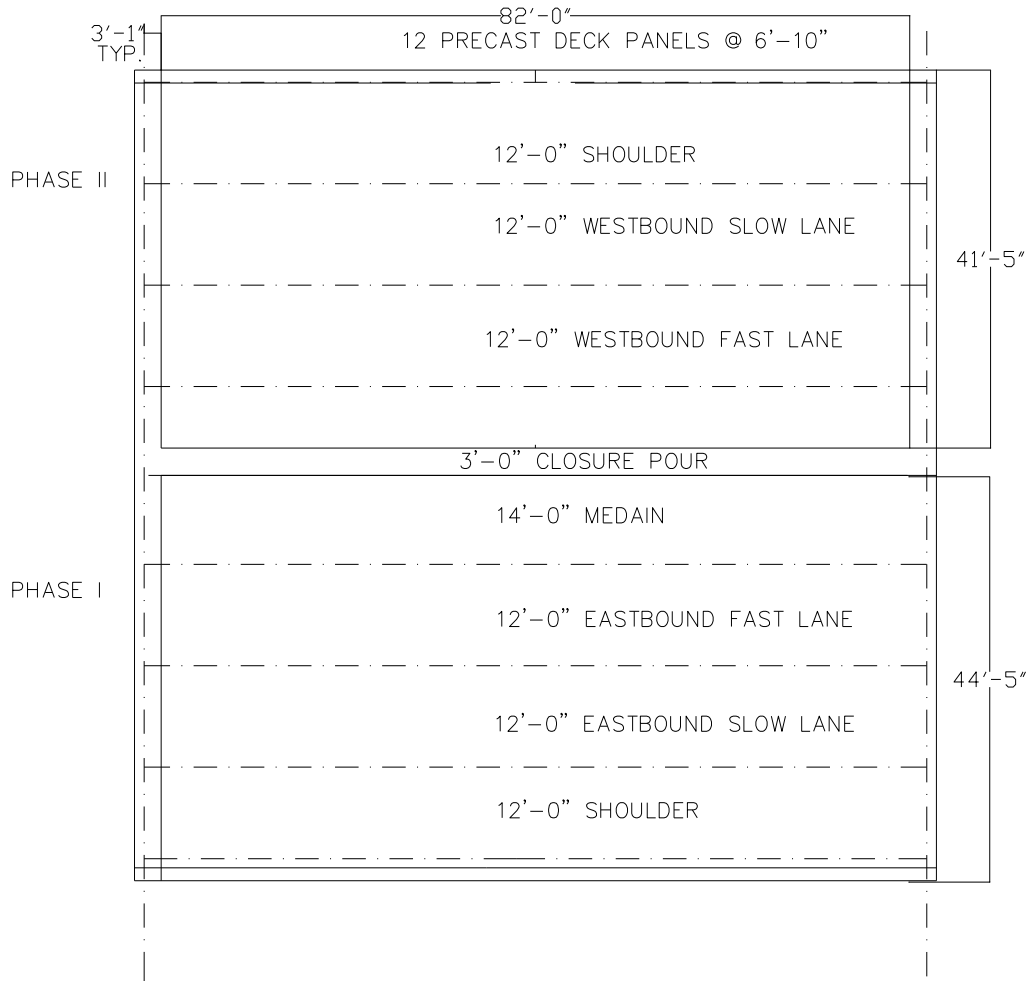


**Figure 2. Plan of bridge**

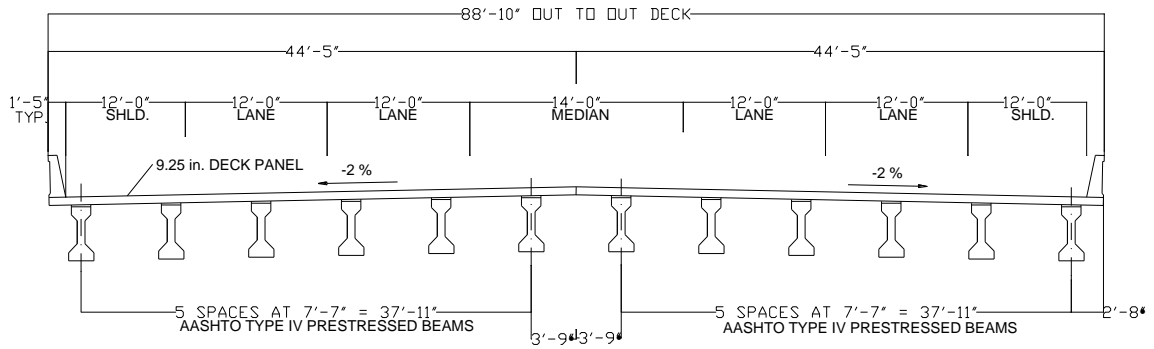


**Figure 3. Bridge cross section looking east**

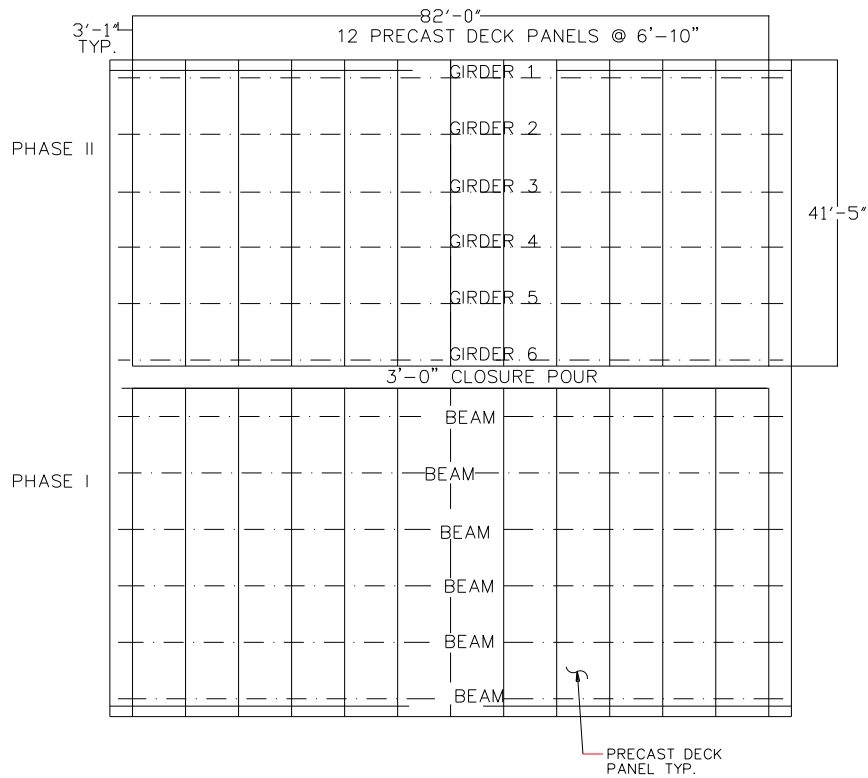


**Figure 4. Bridge plan showing panels and girders**



**Figure 5. Panel EP3 sitting in the precast yard with approach slab rebar to the right**

The 24 deck panels were fabricated in Pleasant Grove, Utah, transported 64 miles to the bridge site, and lifted into place. Each panel was lifted a total of 3 times before ending in its service position. During the first lift, the deck panel was removed from its formwork. This lift took place before the parapet had been cast. Once the parapet had been cast, the panel was placed on the bed of a tractor trailer. During the final lift, the panel was placed on the bridge girders.

Once the panels were in place, they were vertically adjusted using leveling bolts. Once adjusted, the panels were connected to the girders using shear studs and non-shrink grout in the shear stud blockouts to provide composite action with the girders, as seen in Figure 6. Finally, the 3-foot closure pour was cast to connect the 2 sets of panels, as shown in Figures 2 and 4. The deck panels were post-tensioned in the direction of traffic flow, to increase the shear transfer of the grout key between the panels, to reduce the potential for cracking, to close the joints and prevent future leaking. The stress intensity at which the post-tensioning strands were tensioned was only 40.8 kips as compared to the typical jacking force of 46.9 kips.



**Figure 6. Leveling bolts and shear stud blockouts**

## **1.1 Overview of Glass Fiber Reinforced Polymers Bars**

Glass Fiber Reinforced Polymer bars are a substitute for traditional steel reinforcement, and at the most basic level the material is similar to the fiberglass used widely today. GFRP bars are made from long strands of high strength E-glass, (alumino-borosilicate). The strands are bound together with S-glass (alumino silicate). The 2 types of glass fibers together with additives and fillers are combined with a vinyl ester resin in a pultrusion process to create the bars shown in Figure 7. This process is combined with an in-line coating process to obtain exterior adhesion properties (Tang, 1997).



**Figure 7. Close-up of GFRP bar**

Glass Fiber Reinforced Polymer bars offer many advantages over traditional steel reinforcement. The first is corrosion resistance; GFRP bars will not oxidize or change their chemical makeup, they are impervious to the action of salt ions, and the alkalinity inherent in concrete. Corrosion resistance is the biggest factor in reducing long-term costs of bridge decks, and is also the primary reason GFRP bars are chosen for a given application.

The second advantage is their weight. GFRP bars are lightweight, having a unit weight of 135 lbs/cu. feet or approximately one fourth that of steel bars. This offers increased usability and savings in both handling and placement. GFRP bars are void of any metallic substances and are non-conductive. This means that GFRP bars are electromagnetically neutral and will not interfere with the operation of sensitive electronic devices such as medical MRI units or

electronic testing devices. Lastly, GFRP bars do not conduct heat in the same way as steel bars, making them a thermal insulator by comparison (Tang, 1997).

GFRP bars have a few disadvantages when compared with traditional steel reinforcing bars. GFRP bars are more expensive than traditional steel reinforcement. However, their application is specialized. Using GFRP bars in a bridge deck may only increase the cost the bridge by approximately 4% (Benmokrane et al. 2006). As a comparison, the cost of using GFRP bars for the Beaver Creek Bridge increased the total cost of the bridge by 8% (Nix 2010).

The second disadvantage of GFRP bars is their low modulus of elasticity. GFRP bars have a modulus of elasticity equal to 6,280 thousand pounds per square inch (ksi), about one fifth that of steel. The lower modulus means that slabs and structures built with GFRP bars will have higher deflections. For deflection limit-based design, the number of bars in a given structure typically has to be increased to maintain the same deflections as those with steel reinforcement (Liu, 2011).

Another disadvantage of GFRP bars is their inability to be altered in the field. GFRP bars cannot be bent after they have been cured and since they are shipped in a fully-cured form they cannot be bent onsite. Bends can however be produced during the manufacturing process in virtually any shape that can be obtained with steel rebar; however a more generous bend diameter is required. Furthermore, planning for all bends will have to be taken into consideration ahead of construction, and change orders involving GFRP bars are typically more expensive than those involving steel.

## 1.2 Material Properties of GFRP Bars

The properties of the GFRP bars used in the Beaver Creek Bridge were provided by the manufacturer and are summarized in Table 1 (Hughes Bros, 2009). Table 2 offers a comparison of typical properties for GFRP and steel bars. From this table the weight and tensile strength advantages of GFRP bars are obvious. One can also see the advantage steel bars have over GFRP bars regarding the elastic modulus.

**Table 1. Material properties of GFRP bars used at the Beaver Creek Bridge**

Tensile strength average	103,700 psi
Modulus of elasticity	6,280,000 psi
Ultimate Strain	0.0165 inches/inches

**Table 2. Comparison between Aslan 100 GFRP & Grade 60 Steel**

	Units	GFRP Bars Used	Grade 60 Steel
Tensile Strength	ksi	103.7	80
Modulus of Elasticity	$\times 10^3$ ksi	6.28	29
Specific Gravity	Unitless	2.0	7.85
Strain at Failure	%	1.65	6-12
Thermal Conductivity	Btu-in/(feet <sup>2</sup> hr F)	5	360

Under compressive loads, GFRP bars can achieve approximately half their tensile strength, while maintaining their modulus of elasticity. In compression, 3 failure modes are possible: crushing, buckling, and combined buckling and crushing. The modulus of elasticity of GFRP bars in compression is approximately the same as in tension (Deitz et al. 2003).

### **1.3 Design of Bridge And Changes In Design To Accommodate GFRP Reinforcement**

The design of the deck panels was controlled by limiting crack width and deflection. The low modulus of elasticity of GFRP bars may lead to wider crack widths than with traditional steel. The acceptable crack width tolerances can be relaxed with GFRP bars due to their non-corrosive nature. However, the wider crack widths can lead to loss of aggregate interlock and a reduction in shear capacity. GFRP reinforcement also exhibits higher deflections than steel. Due to these design limitations, several adjustments had to be made to the structural design. The first adjustment was to bar spacing; in the transverse direction, spacing was reduced from 8-inches. (203mm) to 4-inches. (102mm) effectively doubling the numbers of bars. This adjustment was the direct result of the low modulus of elasticity of GFRP bars and was based on deflection calculations. The design strength of the concrete was 4000 psi; tested core samples had a strength of 6200 psi. If the strength would have been guaranteed to be 6200 psi, then the number of bars could have been decreased.

It was not economical to increase the number of bars any further, so alternative methods for decreasing crack width and deflection had to be used. A balance between increasing the

thickness of the deck and decreasing girder spacing was used. The deck thickness was increased from the standard 8  $\frac{3}{4}$  inches, to 9 $\frac{1}{4}$  inches. The girder spacing was decreased from 9 feet - 4 inches, to 7 feet - 7 inches, increasing the number of girders from 10 to 12 (Nix 2010). The GFRP reinforcing method posed some additional challenges. Traditional deck panels are lifted and positioned using embedded anchors. However, due to the low shear capacity of GFRP bars, the panels had to be lifted using straps which wrapped around the panel supporting them from below. This made the positioning process awkward, time consuming, and difficult (Nix 2010).

Moreover, the GFRP bars could not provide enough shear strength for post-tensioning stresses at the anchors. To compensate for this, supplementary steel reinforcement was used on the end panels to provide additional strength to the post-tensioning anchors and aid in stress distribution, as shown in Figure 8. Additionally, extra GFRP bars were used to reinforce the area around the post-tensioning anchors (Nix 2010).

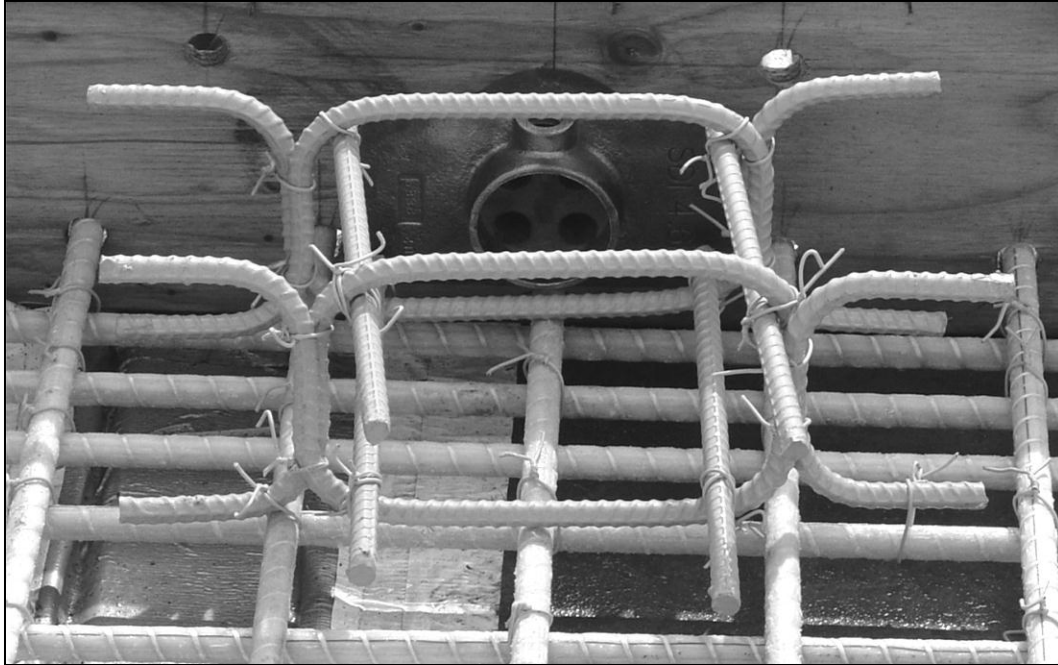


**Figure 8. Steel reinforcement to accommodate increased shear demand from post-tensioning anchor**

The reinforcement consisted of #5 GFRP bars spaced at 4-inches in both the transverse and longitudinal directions and in both the top and bottom mats. The concrete used for the precast concrete panels had a 28-day compressive strength of 6,200 psi. The AASHTO HL-93 design truck was used in the design of the bridge. This loading is the combination of either a design tandem (2 axles at 25 kips/axle and spaced 4 feet apart) or the HS20-44 design truck along with a distributed lane load of 0.64 kips/feet.

## **2.0 EXPERIMENTAL DESIGN**

This Beaver Creek Bridge project attempted to accomplish a number of goals related to health monitoring. The goals can be separated into two categories; monitoring during the construction phase, and post-construction monitoring to be accomplished once the bridge opened. The tasks included:

1. Instrumentation of 2 bridge deck panels associated with Phase II of the Beaver Creek Bridge. Obtaining and reporting data in real time during 3 panel lifts, as well as during transportation. Instrumentation of the Beaver Creek Bridge girders and diaphragms with several sensors. Instrumentation of the bridge site with a still camera, atmospheric sensor, and antenna. Installation of data loggers for automatic data acquisition.
2. Monitoring the 2 panels during every move from initial casting to final placement. Strain data was taken using embedded electrical strain gauges attached directly to the GFRP bars.
3. Comparing the measured curvature diagram from lifting provided by the electrical strain gauges with an analytical curvature diagram.
4. Recording strains during the post-tensioning process using the vibrating wire strain gauges. Comparing the theoretical post-tensioning strains with those recorded from the sensors.
5. Performing static and dynamic truck load tests in which the west-bound lanes would be tested independently as well as simultaneously. The truck load tests gathered data on

girder deflections at midspan, panel deflections between girders, peak vertical accelerations of girders at midspan, and internal strains in the concrete.

6. Determining whether the changes made to the design of the bridge to accommodate GFRP bars were successful in preventing the deck from cracking and maintaining small service deflections.
7. Determining if a trend exists from the accelerometer data relating truck speed to maximum acceleration.
8. Modeling the bridge using finite element methods.
9. Long term health monitoring of the bridge measuring concrete strains, bridge deflections, and vertical accelerations of the girders.
10. Making comparisons of accelerometer data from trucks with known weight and speed.
11. Comparing the cost of the GFRP reinforced deck to a traditional steel reinforced concrete deck.

## **2.1 Experimental Setup**

Due to the decreased elastic modulus of the GFRP bars, the deck had to be lifted using straps instead of embedded anchors as shown in Figure 9. Typically, embedded anchors are attached to the bars; due to the nature of the GFRP bars, the shear capacity of the bar was a concern in the lifting process. Therefore, the panels were lifted from below. For each lift, the panels were lifted at 4 points. Strap locations are shown in Figures 9-10. Figure 10 shows the Prestressed Concrete Institute (PCI) lifting points and the actual lifting points for 3 lifts.



**Figure 9. Panel P2-05 being lifted using straps at the bridge site**

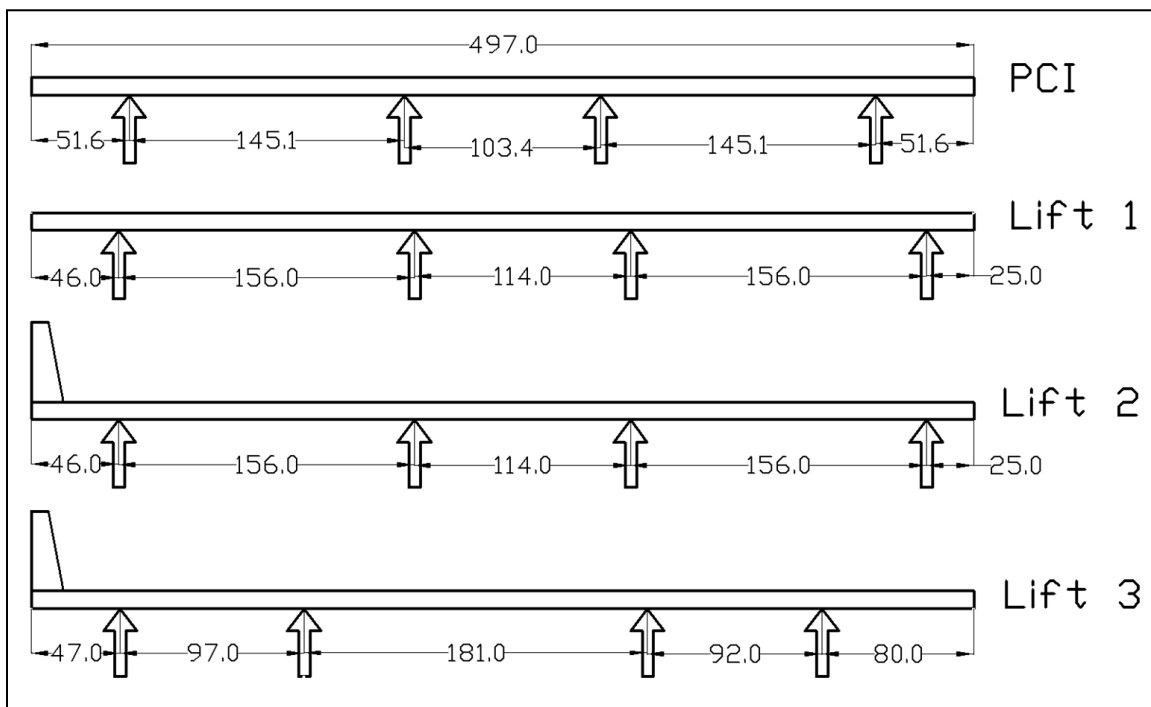


**Figure 10. Lifting point diagram (all dimensions in inches)**

The initial truck load tests (TLT) before the bridge opened to traffic consisted of 9 static tests and 6 dynamics tests, all performed on the west-bound bridge on September 29, 2009. Tests 1-3 were performed on the slow lane using truck “A”. Tests 4-6 were performed on the fast lane using truck “B”. Tests 7-9 were a combination of tests 1-3 and 4-6 respectively, and used both trucks with Truck “A” in the slow lane and Truck “B” in the fast lane. Table 3 provides details of

the weight of trucks “A” and “B” as well as the HL-93 design vehicle. Table 4 provides an overview of the static tests performed. Figure 11 provides the dimensions of the 2 test trucks and Figure 12 provides details about each of the tests. 3 types of data were recorded for each of the static truck load tests: midspan girder deflections, panel deflections relative to the girders, and concrete strains in both the transverse and longitudinal direction of the bridge. A second static truck test occurred on September 1, 2010; both “A” and “B” trucks were placed simultaneously over the girders in 5 different stations: (1) east abutment, (2) east diaphragm, (3) midspan, (4) west diaphragm and (5) west abutment. The truck weights were similar to the previous test in order to compare long term data.

**Table 3. Truck Weights**

Truck	Weight-kips	Rear Axle-kips	Front Axle-kips
A, 2009	43.88	14.78	29.10
B, 2009	43.16	14.48	28.68
A, 2010	37.94	14.5	23.44
B, 2010	45.68	17.48	28.2

HL-93 Design Truck Axle Weight (lbs)

Front axle	8000
1 <sup>st</sup> Rear axle	32000
2 <sup>nd</sup> Rear axle	32000
Gross WT	72000

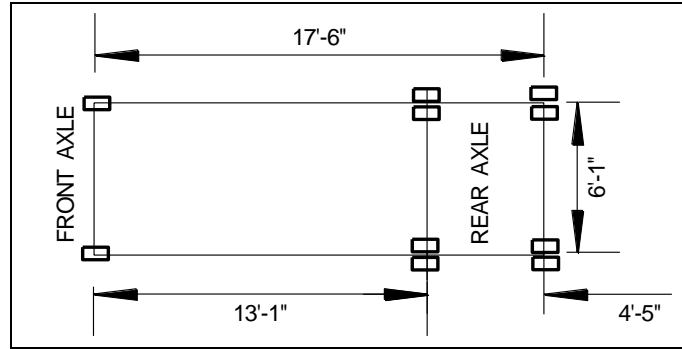


**Figure 11. Test truck dimensions**

**Table 4. Static Tests**

Test #	Type of test	Lane Tested	Truck used	Rear Axle Position
1	Static	Slow	A	East Diaphragm
2	Static	Slow	A	Midspan
3	Static	Slow	A	West Diaphragm
4	Static	Fast	B	East Diaphragm
5	Static	Fast	B	Midspan
6	Static	Fast	B	West Diaphragm
7	Static	Both	A&B	East Diaphragm
8	Static	Both	A&B	Midspan
9	Static	Both	A&B	West Diaphragm

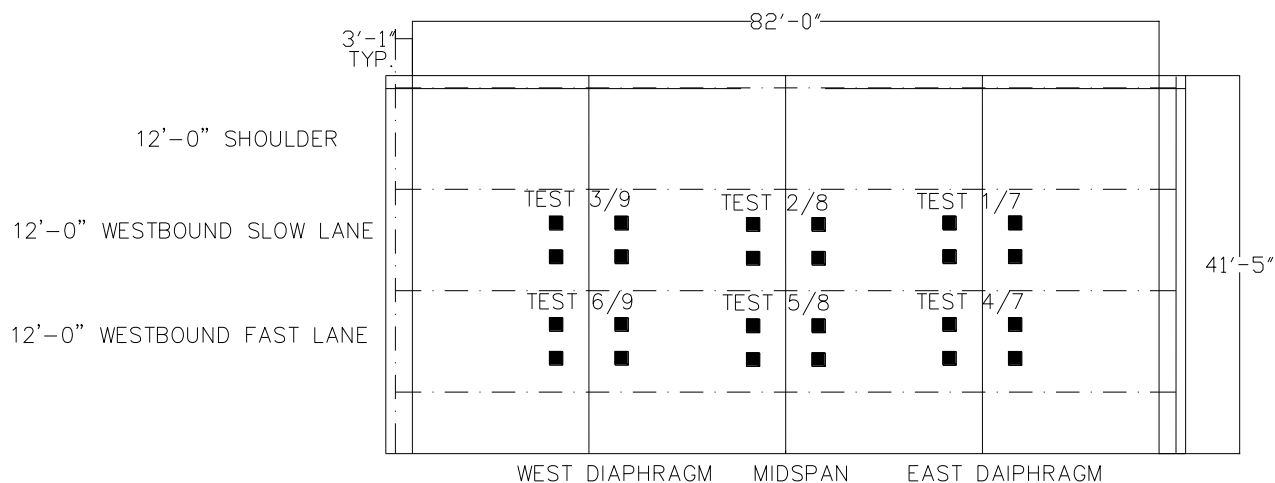


**Figure 12. Locations of trucks during truck load test**

Truck Load Tests 10 - 15 in the first truck load test (Sept. 29, 2009) were dynamic tests, with trucks “A” and “B” driving westward in the west bound direction of the bridge. Tests 10 -11 were conducted at 40 miles per hour (mph) with each truck in its lane. Test 12 was performed with both trucks simultaneously traveling at a speed of 35mph. Tests 13 - 14 were faster versions of Tests 10 - 11 and were conducted at 65mph. Test 15 was not conducted due to safety concerns about the length of stopping distance for the two trucks. The dynamic truck load tests are summarized in Table 5. Dynamic truck load tests carried out on September 1, 2010 were of a similar fashion. Truck A was positioned in the slow lane with a weight of 37.94 kips while Truck B was in the fast lane at 45.68 kips. A third dynamic truck load test was performed on November 19, 2010 with a truck weighing 65.9 kips. The truck was positioned in the slow lane and, due to the type of truck, it could only reach a maximum speed of 55 mph. This heavier truck was important for testing purposes to observe how the bridge responds to a heavier load and if there is a relationship between girder response and weight. A fourth test was conducted on November

21, 2011, which was an ambient traffic test with trucks of a known weight; the truck speed was measured by a Pro Laser III LiDAR gun.

**Table 5. Initial Dynamic Test Details at Bridge Opening**

Test #	Type of test	lane tested	Truck used	Velocity (mph)
10	Dynamic	Slow	A	40
11	Dynamic	Fast	B	40
12	Dynamic	Both	A&B	35
13	Dynamic	Slow	A	65
14	Dynamic	Fast	B	65
15	Dynamic	Both	A&B	Not preformed

## 2.2 Instrumentation Setup

2 panels were chosen for instrumentation due to their location on the bridge, End Panel Three (EP3) is located next to the west abutment of the bridge and Phase 2 Panel Five (P2-05) is located at the mid-span of the bridge, as shown in Figure 13. This project used 2 types of strain gauges for monitoring the strains inside the panels. Displacement sensors were also used for monitoring the performance of the panels, accelerometers were used to monitor peak accelerations of the bridge girders at midspan. Furthermore, 1 sensor was used to monitor the atmospheric conditions at the bridge site. In addition to the 5 sensors mentioned above, surveying equipment was employed to determine the midspan deflection of the girders during the static load test.

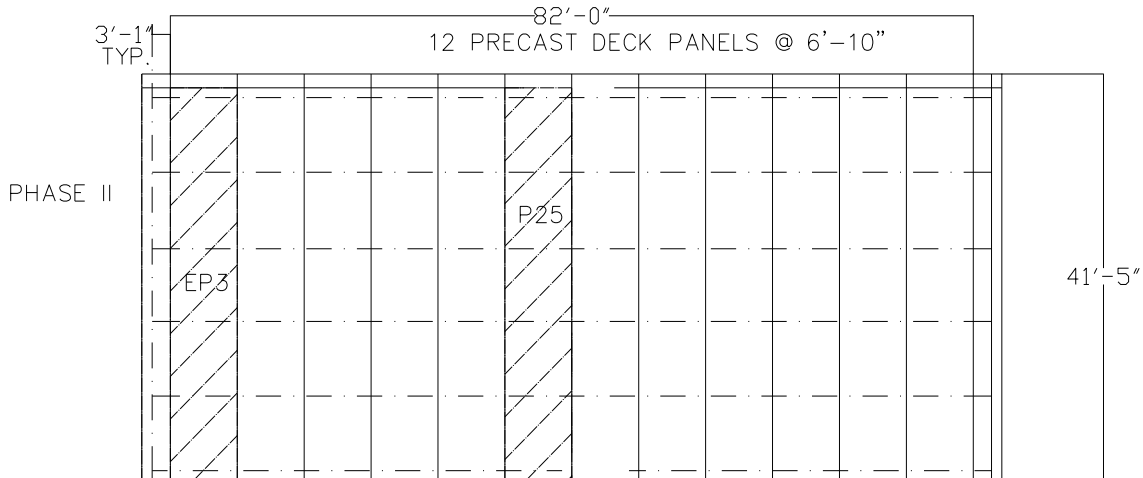


**Figure 13. Plan of bridge with instruments and panel**

### 2.2.1 Electrical Strain Gauges

Each panel was instrumented with 28 electrical strain gauges, to be used during lifting and transportation of the panels. These gauges were attached directly to both the top and bottom GFRP mats and recorded the strains in the bars. Of the 28 gauges, 20 were placed in the transverse direction of the bridge (longitudinal direction of the panel) to record strains in the long dimension of the panel during lifting. The remaining 8 gauges were placed in the longitudinal direction of the bridge to record strains in the short dimension. Figure 14 provides a more detailed look at the locations of the gauges. Gauge locations were chosen due to their proximity to the lifting points and point of maximum theoretical moment. Electrical strain gauges were chosen due to their high sampling rate potential, relatively low cost, and overall simplicity. Drawbacks include difficulty in attaching them to GFRP bars, as well as their short life span.

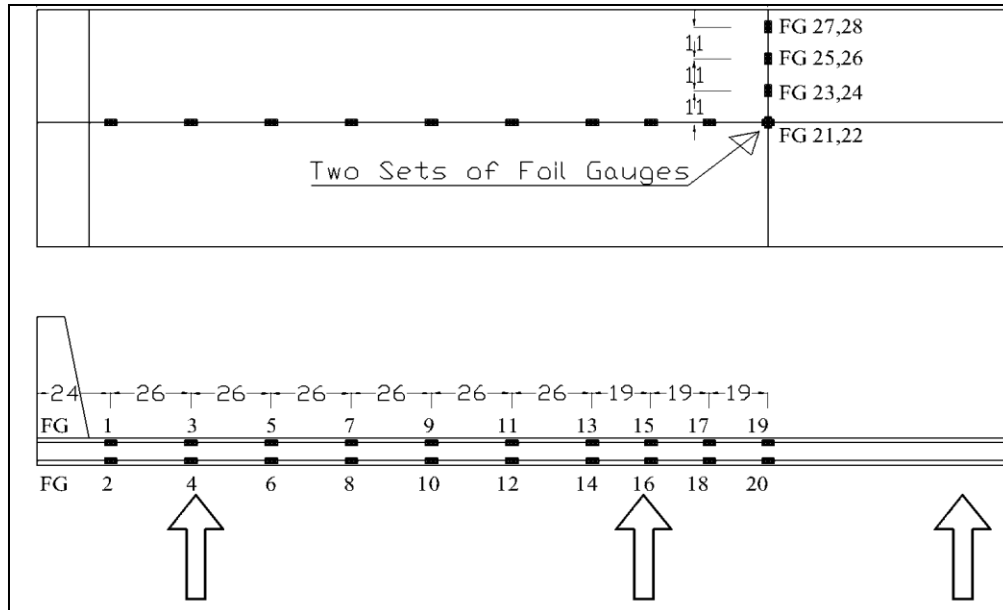


**Figure 14. Electrical gauge locations for both panels**

## 2.2.2 Vibrating Wire Strain Gauges

Panels EP3 and P2-05 were instrumented with 4 vibrating wire strain gauges (VWSG) placed in the longitudinal direction of the bridge. These gauges were used to record strains in the concrete induced by post-tensioning as well as the change in strain due to creep and other long term effects.

In addition to the 4 longitudinal VWSGs, panel P2-05 was equipped with 16 additional VWSG placed in the transverse direction of the bridge, as shown in Figure 15. These gauges were primarily used during the truck load test and for long term monitoring. Gauge locations were chosen due to their proximity to the girders and location of the truck during the truck load test. The advantages of VWSGs include long life, built-in thermistor and ease of installation; however, they have a relatively low sampling rate.

The VWSG were secured to the GFRP mats using zip ties and foam blocks and lie in the same horizontal plane as the GFRP mats, as shown in Figure 16. Each of the VWSGs has a built-in thermistor which records the temperature of the concrete in the panel. The maximum sampling rate for a VWSG is approximately 2 seconds and the sampling is carried out 1 sensor at a time.

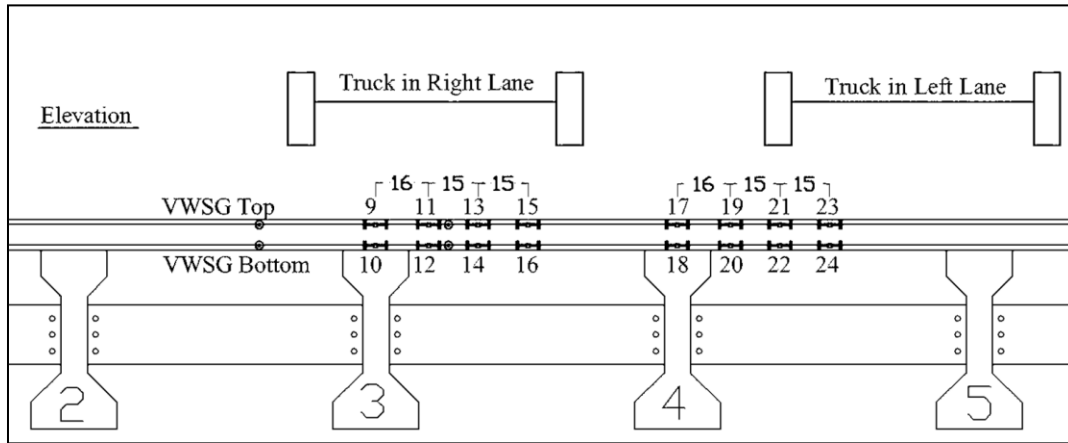


**Figure 15. Vibrating Wire Strain Gauge locations**

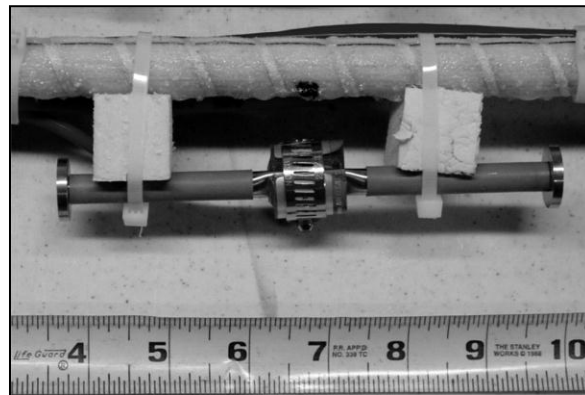


**Figure 16. Close up of Vibrating Wire Strain Gauge attached to GFRP rebar**

### 2.2.3 Linear Variable Differential Transducer (LVDT)

The bridge was instrumented with 6 LVDTs. These sensors were placed on top of the diaphragms midway between the girders to measure the deflection of the deck relative to the girders. LVDTs #1-#5 were placed above the west diaphragm between girders 1 -6 respectively. LVDT #6 was placed between the second and third girder above the east diaphragm, directly across from LVDT #2. The LVDTs were attached to the diaphragms using hose clamps and a piece of square bar welded directly to the diaphragm, as shown in Figure 17.



**Figure 17. Linear Variable Displacement Transducer attached to diaphragm under bridge**

#### **2.2.4 Accelerometers**

The bridge was instrumented with 6 single-axis accelerometers. The accelerometers were attached to the bottoms of girders 1-6 at midspan of the bridge to measure vertical accelerations. They were used during truck load tests to obtain peak accelerations, during long term monitoring for the collection of acceleration signatures and the triggering of the camera. The accelerometers have a sampling rate of 50Hertz and a sensitivity of 0.001g.

### **2.2.5 Atmospheric**

Atmospheric data was collected using an HMP-50 sensor from Campbell Scientific. The sensor was mounted to a fence post adjacent to the bridge as shown in Figure 18. Data was averaged and recorded every 12 hours. The HMP-50 records both relative humidity as well as temperature. The accuracy of the relative humidity sensor is  $\pm 3\%$  (0% to 90% range) and  $\pm 5\%$  (90% to 98% range); the temperature sensor has a range of  $-40^{\circ}$  to  $+60^{\circ}\text{C}$  and is accurate to within 0.1 degree.



**Figure 18. HMP-50 in its protective housing attached to fence post adjacent to bridge**

### **2.2.6 Surveying Equipment**

In addition to the 5 types of sensors mentioned, surveying equipment was used to determine the midspan deflection of the 6 girders for each of the 9 static truck load tests. A Sokkia SLD30 power level was operated with a RAB (Random Bi-directional) code elevation staff to provide the deflections of the girders. The staff was held against the bottom of the girder by an operator in a JLG lift positioned under the bridge, as shown in Figure 19.

### 2.2.7 Camera

A still camera was aimed toward the bridge as shown in Figure 20; it was mounted on a 15'-0" post stationed approximately 30 feet north of the west abutment as shown in Figures 21-22. The purpose of the camera was to obtain a visual record of the truck that caused the largest accelerations. The camera is triggered whenever accelerometer #5 reaches a specific threshold of 0.025g.



**Figure 19. Surveying team for truck load test**



Figure 20. Still camera used for visual record of truck causing large accelerations

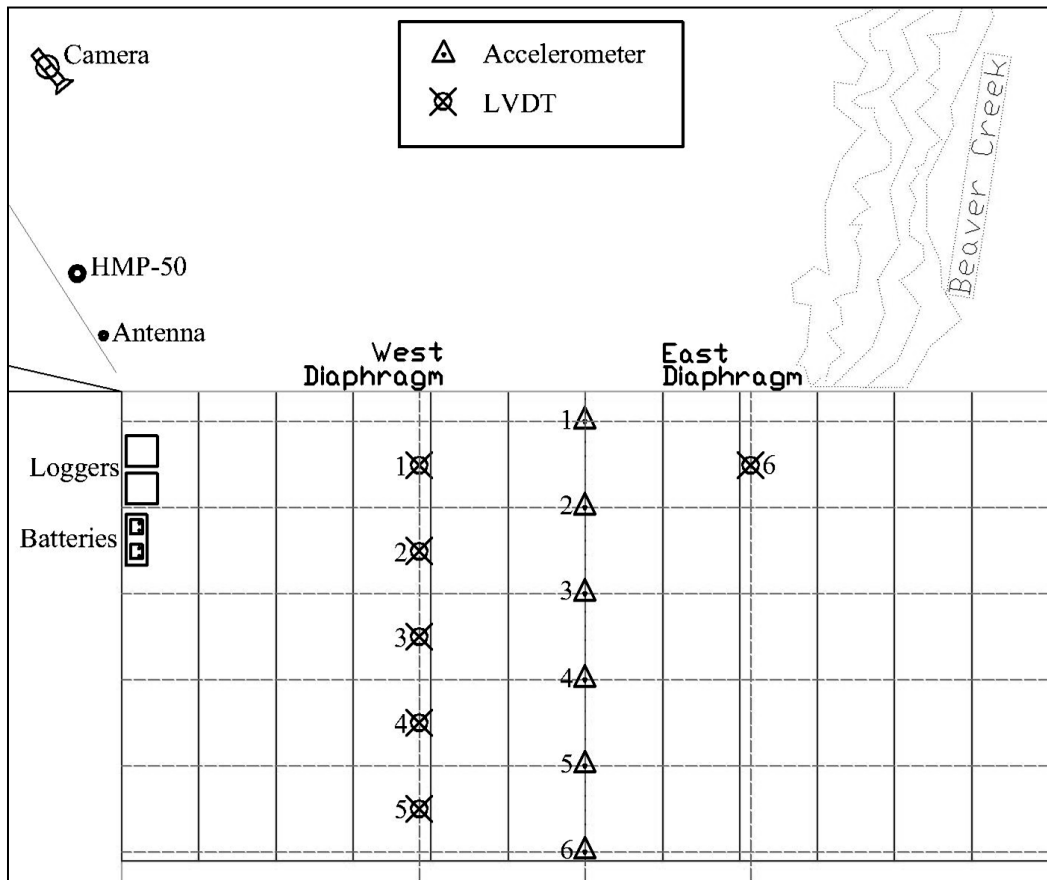


Figure 21. Instrument locations on the bridge



**Figure 22. Location of camera with respect to bridge**

### **2.3 Data Acquisition and Remote Data Transfer**

Data for this project was recorded using 1 of 3 data loggers; occasionally data had to be taken manually. This section provides a brief overview of the equipment used during this project and the different setups for data acquisition and transfer.

Three data loggers were used in this project: 2 CR3000 Microloggers® and 1 CR1000 Measurement and Control Datalogger. The 2 CR3000 Microloggers were designated “A” and “B”. This project also used 3 RF401 900-MHz Spread-Spectrum radios for transmitting real-time data from the loggers to the laptop during panel lifting and moving procedures. An AVW200 Vibrating-Wire Interface was used for exciting and measuring the VWSGs. 3 AM16/32a 16-channel or 32-channel Relay Multiplexers (MUX) were used to increase the

capacity of simultaneously connected sensors. The specifications of the above mentioned equipment can be found on the Campbell Scientific™ website.

During this project the three data loggers were used in four different arrangements. The first setup was for initial lifting of the panels, removing them from the formwork. Here both CR3000s were used to collect strain gauge data from the electrical strain gauges at a sampling rate of 10 Hertz. Each CR3000 is capable of collecting data from 14 electrical gauges. The data was recorded in the memory of the logger but also broadcast in real time to an onsite laptop via a network of RF401 radios, as shown in Figure 23.

During the second setup, the 2 instrumented panels were transported to the bridge site simultaneously. Each panel was issued 1 CR3000, 1 AM16/32a multiplexer, and 1 RF401. 13 of the 28 electrical strain gauges on each panel were connected directly to the CR3000; the rest were connected to the CR3000 using the multiplexer. The data from both panels was recorded to the memory of the loggers. Panel P2-05 was monitored in real-time during its transportation. Monitoring took place from a van which followed the flat-bed trailer at a safe distance, and communicated with the logger via a network of RF401 radios, as shown in Figure 24.

To record the strains induced by post tensioning, all VWSGs were connected to the CR1000 via the AVW 200 and two multiplexers. The loggers were left running at the site the night before post tensioning began, and retrieved 2 days later. As a backup before and after post tensioning, data was taken manually from the VWSGs using a Geokon GK-401 Vibrating Wire Readout Box. The GK-401 excites the sensor and measures strain. An ohm-meter was used to

measure the resistance in each of the thermistors, which corresponds to temperature. During the post-tensioning only, it became evident that the data recorded on the logger was erratic and the manually taken data from the GK-401 was used instead.

Data acquisition during the truck load test and long term monitoring used very similar setups but used different sampling schemes. The VWSGs data was collected manually for each of the static truck load tests. Baseline data for the VWSGs was also taken. The 6 LVDTs were connected to CR3000A with a sampling rate of 1 Hertz. The CR3000 can only support 4 accelerometers; as a result, the sensors had to be split up with 4 of the accelerometers attached to CR3000A, and the remaining 2 to CR3000B. The CR1000 recorded the atmospheric data taken hourly by the HMP-50. The accelerometers recorded all activity during the dynamic truck load tests at a rate of 50 Hertz. Finally, during each static truck load test, the girder deflections were recorded using surveying equipment. Baseline data was also taken. The truck load test and long term setups are visualized in Figure 25.

The long term data acquisition set up was the same as the truck load test setup with the following exceptions. The data loggers are powered by (2) 12 volt car batteries; the batteries are charged using 2 solar panels and a voltage regulator. The VWSGs were connected to the AVW200 via two AM16/32a multiplexers, the AVW200 was connected to the CR1000 along with the HMP-50, and this data was sampled every 2 minutes, and then averaged and recorded every 3 hours. The sampling rate of the LVDTs remained at 1 Hertz and was averaged and recorded in 3 hour periods. The camera is connected to the CR3000B, the same microllogger used to record accelerometers 5 and 6. The camera is triggered whenever the acceleration of

accelerometer #5 goes above 0.025g. Long term accelerometer data is acquired in 2 ways; first, the datalogger records the largest acceleration each day and the time of day when it occurred; second, whenever accelerometer #5 reads above the 0.025g threshold, a series of data is recorded in which 50 samples before the event and 250 samples following the event are recorded. Together with the camera, this setup provides a picture as well as an acceleration signature every time accelerometer #5 exceeds the 0.025g threshold.

The 3 dataloggers are connected to each other through their COM ports allowing them to communicate with each other. The modem and antenna are connected to CR3000B which allows the laptop to access any of the data loggers from anywhere an internet connection is available, as shown in Figure 26. Remote access via the laptop allows the user to receive and send programs changing the sampling rate or sampling scheme. It also allows the user to collect data stored on the loggers, manually trigger the camera, and monitor any of the sensors or battery voltage in real time.

Remote access is possible by using software on the laptop to communicate with the dataloggers. Many different Campbell Scientific software were used during this project. RT-DAQ was used for monitoring the lifting strains in real time due to its high refresh rate. Loggernet was used for accessing the dataloggers remotely, which provided access to download data tables, upload new programs for the dataloggers to run, monitor the bridge from offsite and manually trigger the camera. The program Ace Manager was used for configuring the camera. 2 programs were used for the compilation of data logger programs, Short Cuts and the CR Basic Editor. Lastly, a program called the Device Configurations utility was used to configure the dataloggers for use with all secondary hardware.

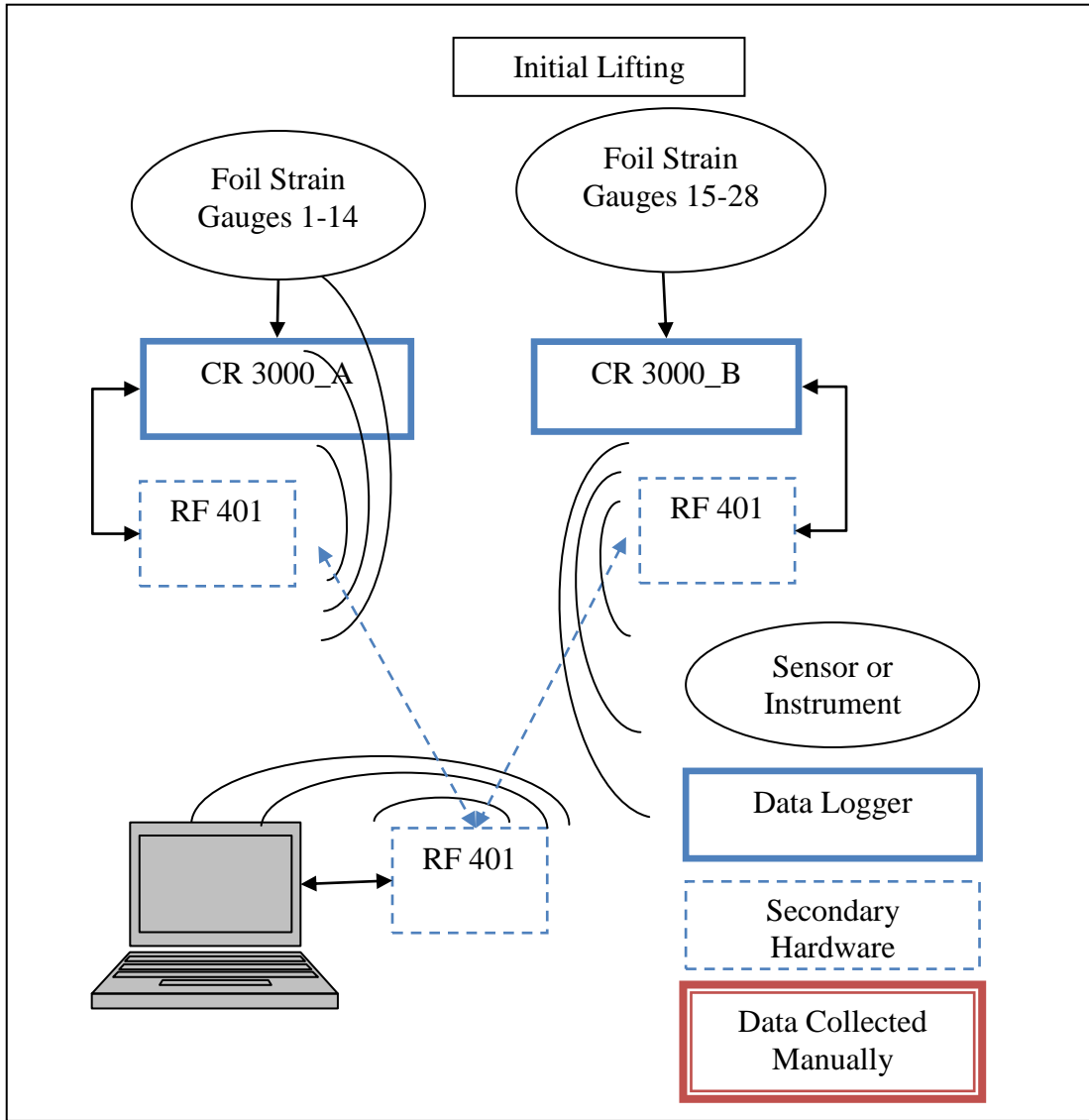


**Figure 23. Equipment setup for initial lifting**

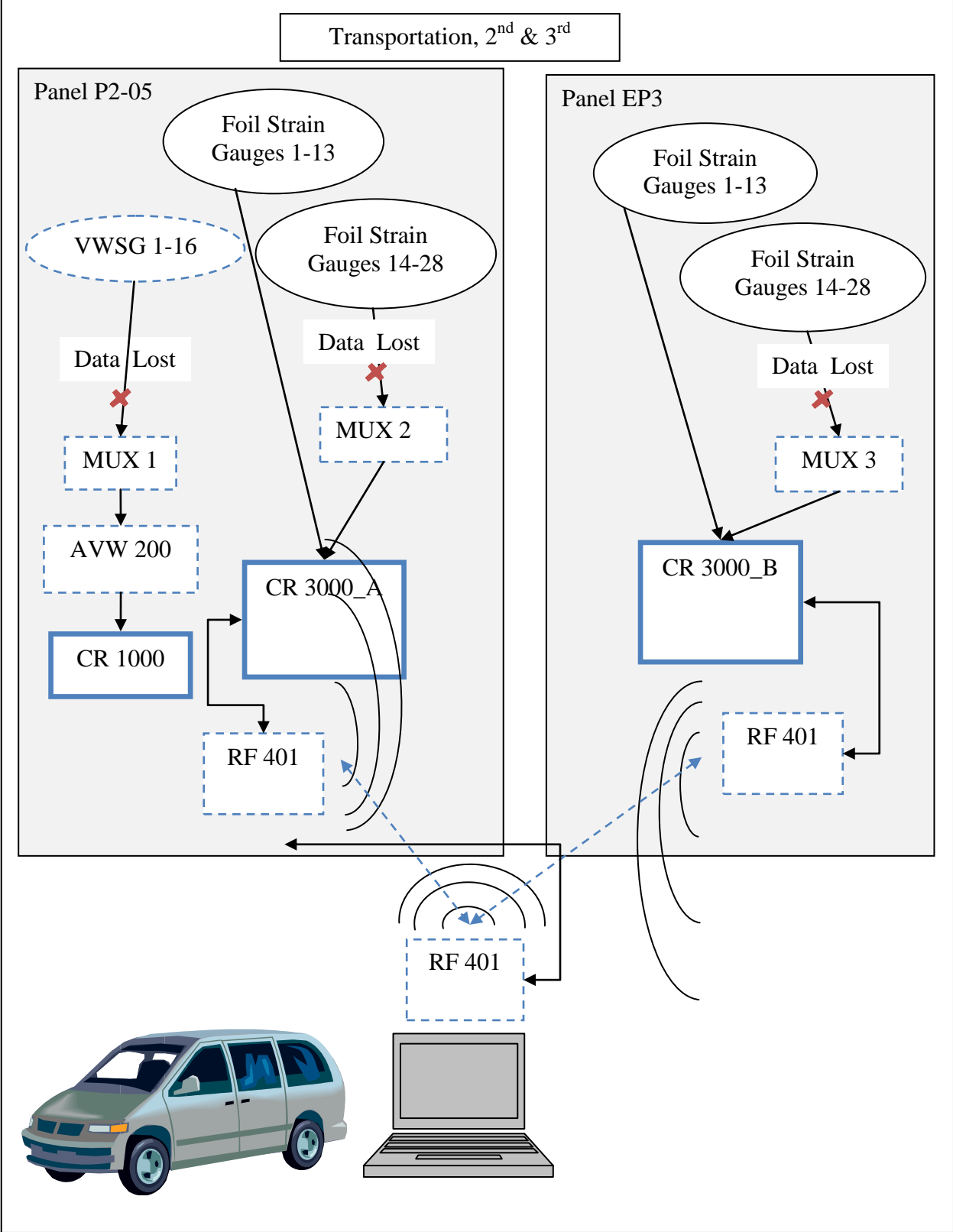


**Figure 24. Equipment setup for transportation, 2nd and 3rd lifting**

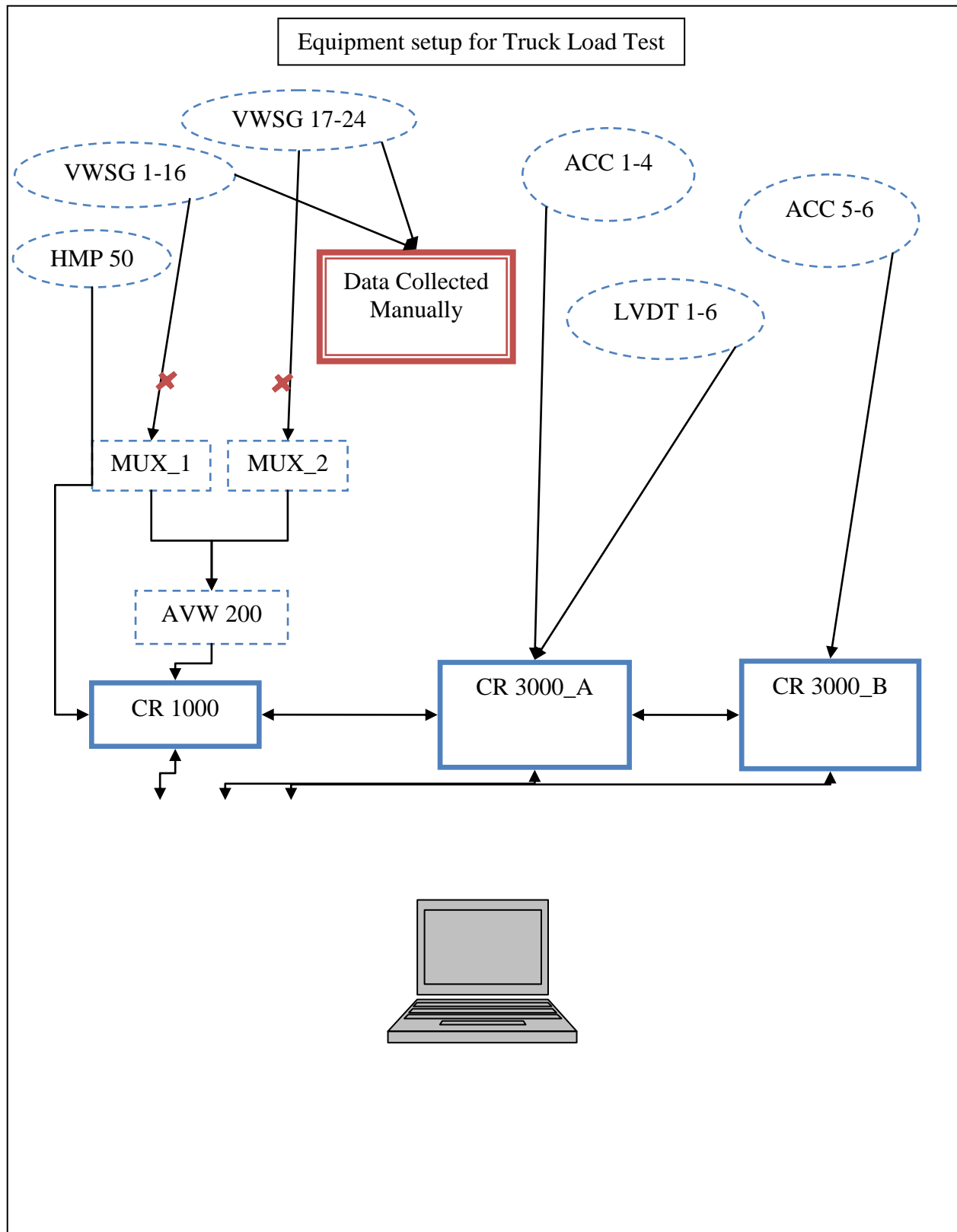
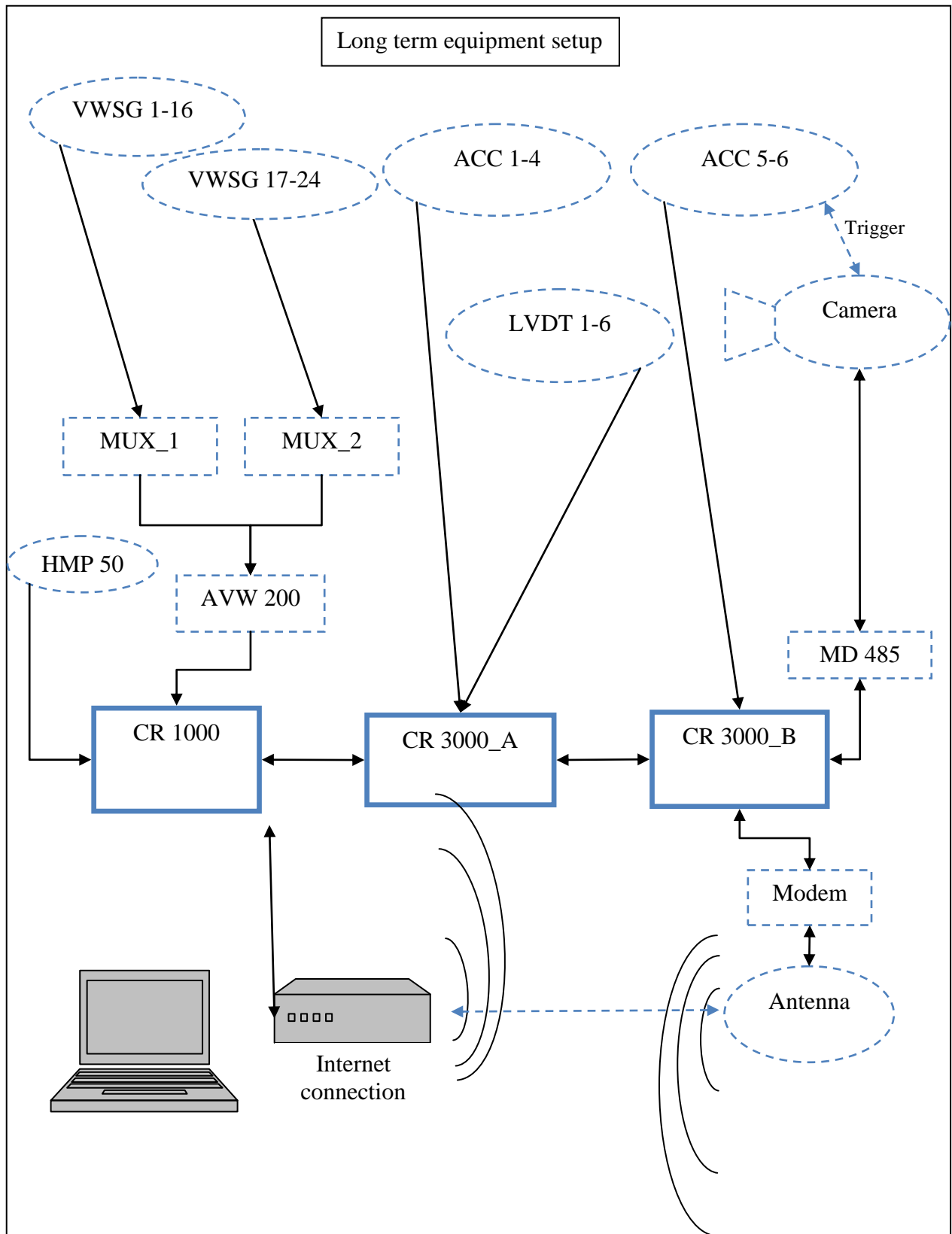


Figure 25. Equipment setup for truck load test



**Figure 26. Equipment setup for long term monitoring**

### 3.0 EXPERIMENTAL OBSERVATIONS

#### 3.1 Experimental Observations for Lifting and Transport

##### 3.1.1 First Lift

Panels P2-05 and EP3, respectively were lifted on July 27<sup>th</sup> and August 6<sup>th</sup> 2009. The lifts occurred before the parapets had been cast. The panels were lifted from the formwork at 4 locations, as shown in Figure 10 (Lift 1). The maximum strain profile for half of the panel P2-05 is shown in Figure 27; one can observe that the maximum strain in the bottom mat is 125 microstrains ( $\mu\epsilon$ ) while the maximum strain in the top mat is 50 $\mu\epsilon$ . The lifting points are located at 46 inches and 202 inches from the left panel edge as shown in Figure 10 (Lift 1), and represented by arrows.

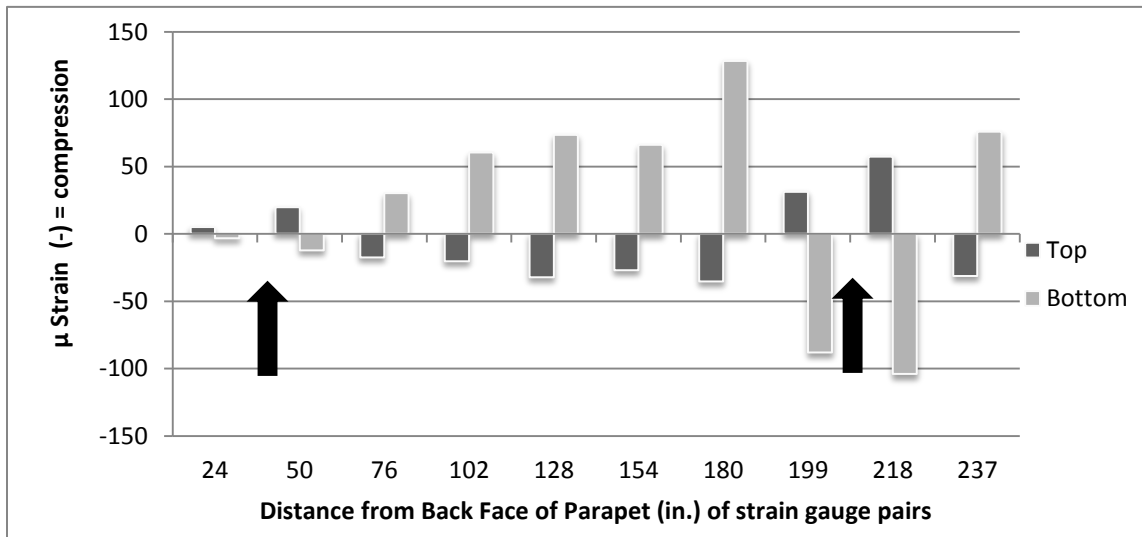


Figure 27. Strain profile for P2-05 during its first lift removing it from the formwork

### 3.1.2 Second Lift

The panels were transported from the precaster to the bridge site on September 3<sup>rd</sup>, 2009. The transportation process involved 2 lifts (referred to as Lifts 2 and 3 as shown in Figure 10), and a 64 mile journey on a flatbed trailer. At this point the parapets on both panels had been cast. The collected data from this day is limited to the first 13 strain gauges from each panel. The maximum strain profile during the second lift for half the panel is shown in Figure 28. From the graph one can observe that the maximum strain in the bottom mat is  $-45 \mu\epsilon$  while the maximum strain in the top mat is approximately  $30 \mu\epsilon$ .

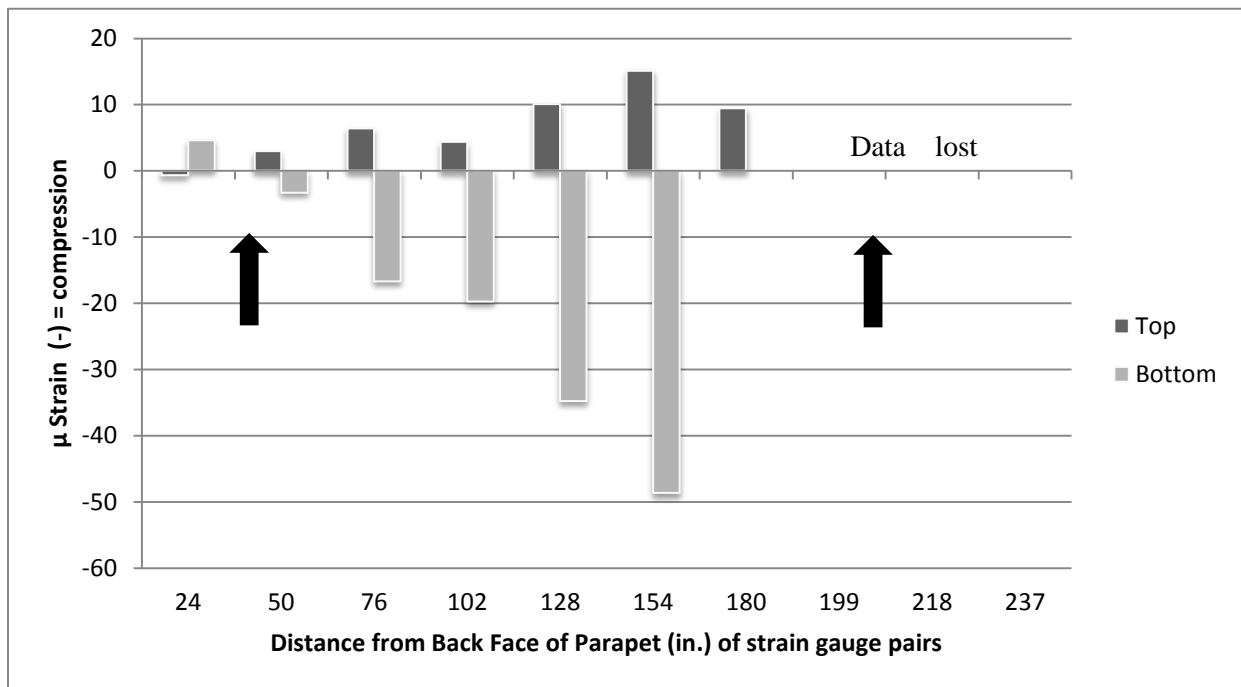
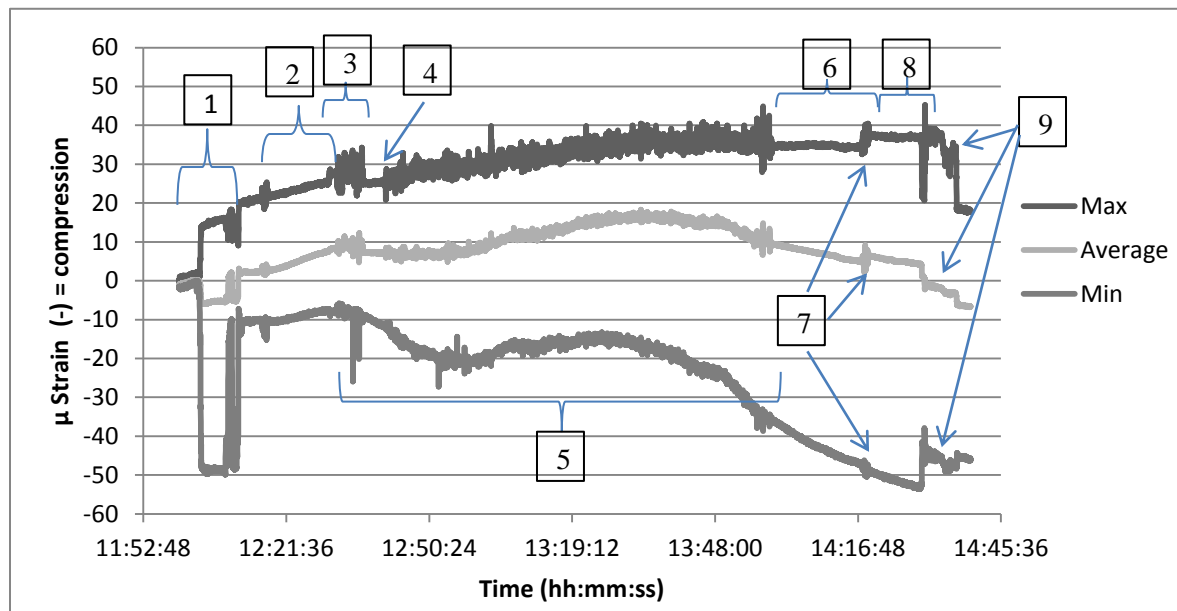


Figure 28. Strain profile for panel EP3 during its second lift

### 3.1.3 Transport

After the panels were placed on the trucks, the trucks began a 64 mile journey to the bridge site. The maximum, minimum, and average of all the strain gauges during the journey is shown in Figure 29. During transport of panel EP3 careful observations were made and correlated to the strains on the graph.



**Figure 29. Max, min, and average strain from all gauges during lifting and transport of panel EP3**

Long term observations, on the order of hours, have resulted in trends that represent the varying nature of the strain during the transportation of the panels. The maximum strain for the entire day did not surpass 60  $\mu\epsilon$  in ether tension or compression. As shown in Figure 29, observations made during the day panel EP3 was moved to the bridge site included:

1. The second lift, placing the panel on the truck.
2. Truck is stationary while panel is strapped down and straps are tightened resulting in slight increase in strain.

3. Truck begins to move through the precast yard and out of Pleasant Grove.
4. Truck is stationary while waiting to get on the freeway.
5. Truck travels the 64 mile distance to the bridge site.
6. Truck arrives at the bridge site and remains stationary until it is unloaded.
7. Truck maneuvers the construction site and moves into position.
8. Straps are removed.
9. Panel is lifted into place during Lift 3.

### 3.1.4 Third Lift

The maximum strain profile during the third lift is shown in Figure 30. The third lift occurred directly after the transportation of the panel to the bridge site; lifting points are shown in Figure 10. From the graph one can see that the maximum strain in the bottom mat is  $-45 \mu\epsilon$  while the maximum strain in the top mat is  $-35 \mu\epsilon$ . The strains for all 3 lifts never exceeded  $125 \mu\epsilon$ .

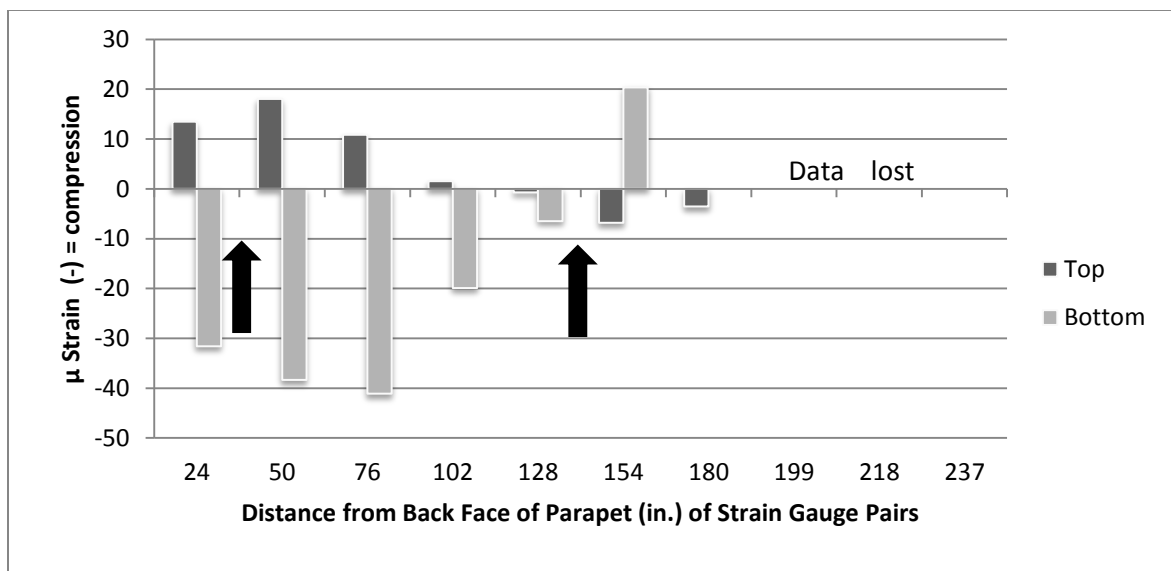


**Figure 30. Strain profile for EP3 during its third lift**

### 3.2 Post-Tensioning Observations

The Beaver Creek Bridge is the first bridge deck using precast deck panels in the state of Utah to be post-tensioned in the longitudinal direction. Post-tensioning of the bridge deck was conducted on September 17, 2009. Post-tensioning consisted of stressing steel strands in 11 pockets. Each pocket contained three 0.6 inches. (15mm) Grade 270 (1862MPa) low relaxation steel strands. Once post-tensioning was completed, the pockets were grouted. Originally, post-tensioning data was to be recorded using the dataloggers, thus allowing for the observation of the post-tensioning process as well as the collection of data for the following days when the majority of immediate losses occur. Due to a wiring error, the post-tensioning data from the loggers was erratic; the before and after data was collected manually. As a result, the data on post-tensioning presented in this paper includes the effects of anchorage losses, elastic shortening and strand relaxation combined.

Before and after post-tensioning, additional data was taken from the VWSGs in the longitudinal direction. The change in strain with temperature adjustment is displayed in Figure 31. The odd numbered gauges are located in the same horizontal plane as the top mat of GFRP reinforcement in the deck panels. The even numbered gauges are located in a similar fashion with the bottom mat. Gauges 1-4 are located on panel EP3 and gauges 5-8 are located on panel P2-05, as shown in Figure 32.

The average concrete strain from all 8 gauges is approximately  $130 \mu\epsilon$  in compression. However, the average concrete strain for panel EP3 is  $112 \mu\epsilon$ , almost  $30 \mu\epsilon$  lower than those found in panel P2-05 where the average strain was  $141 \mu\epsilon$ . Approximately the same difference in

strain was found when comparing the averages of the top gauges to those of the bottom gauges. This difference is most likely due to the eccentric forces in the post-tensioning ducts. 3 tendons were used and eccentrically placed in the panel rather than the planned 4 tendons that could have been easier balanced.

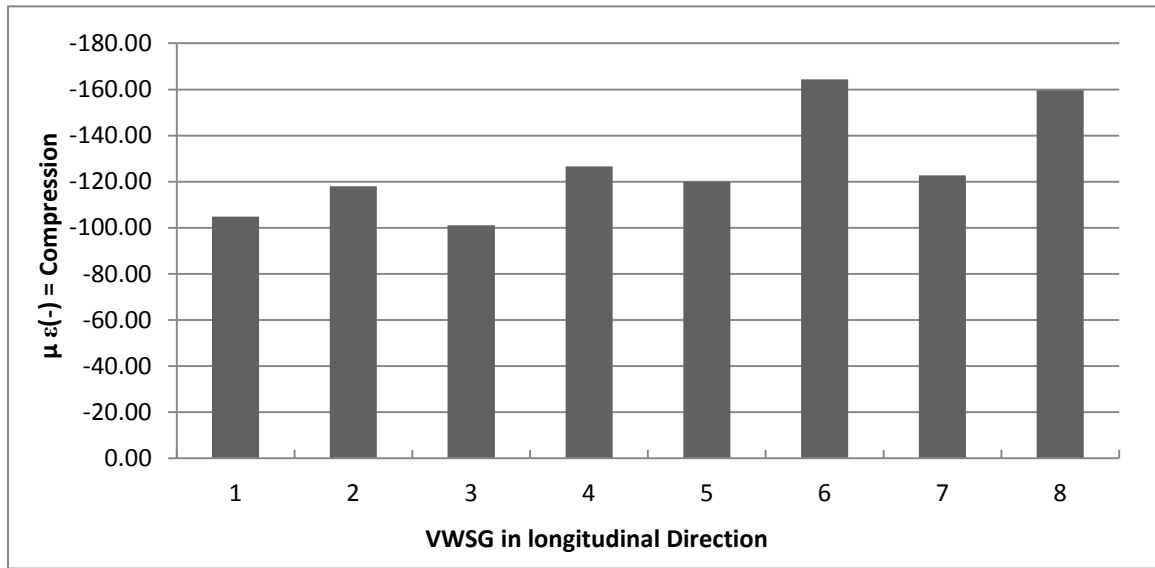


**Figure 31. Post tensioning strains in bridge deck**

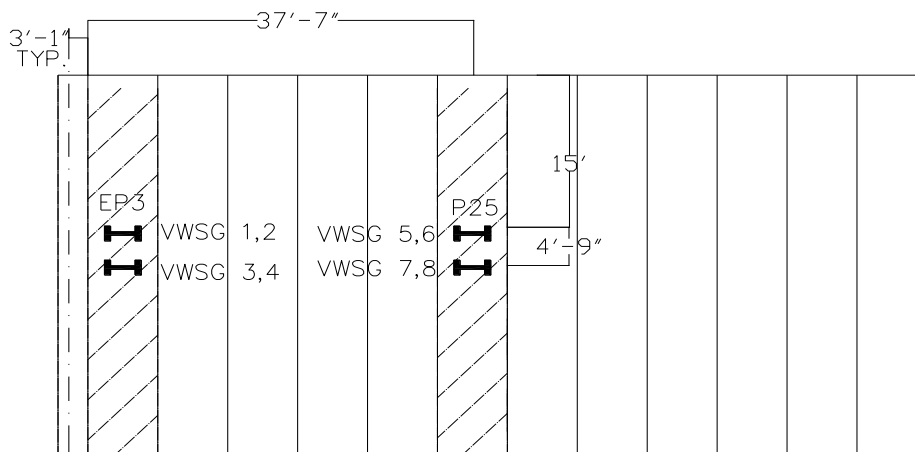


**Figure 32. Locations of VWSGs for measuring strains due to post-tensioning**

### **3.3 Truck Load Test Observations**

The first truck load test was carried out on September 29, 2009 just before the bridge was opened to traffic. The second truck load test was carried out on September 1, 2010 while the west bound bridge was closed to traffic for maintenance operations.

#### **3.3.1 Vibrating Wire Strain Gauges**

The maximum compressive and tensile strains in the concrete occurred during Test 2 when truck “A” was directly over the right lane. The maximum compressive and tensile strains were  $-176 \mu\epsilon$  (microstrain) and  $18 \mu\epsilon$  respectively. The tensile strains observed throughout the static truck load tests were small and only observed at the top of the panel. The majority of the sensors were in compression throughout the truck load tests. The only gauge to exceed  $150 \mu\epsilon$  (tension) was VWSG #20. On the whole, the strains observed in the concrete during the Truck Load Test were not significant. It is believed that the loads were insignificant when compared to the capacity of the deck. The strains observed in the concrete during the truck load test were larger than those observed in the GFRP bars during lifting and transportation of the panels. However, the truck load test strains were still small with respect to the capacity of the deck, which is the intent of the design.

The VWSG for long term monitoring have a mechanical component that measures the change in strain in the concrete and a temperature component that records the 24 hour diurnal strain from morning to night. These 2 components are combined in 1 output. Figure 33 shows a graphical representation of 2 years of true strain in the concrete for VWSG #2, located at the bottom mat of the bars.

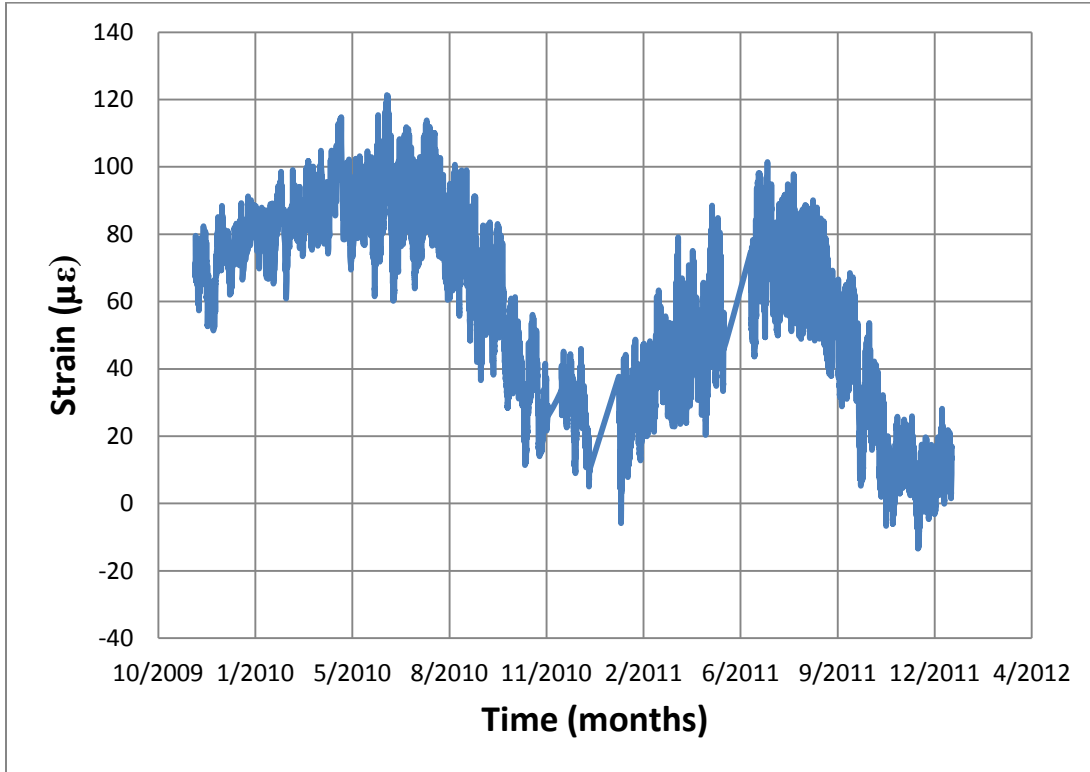


**Figure 33. Two-year concrete strain record**

Separating out the thermal effects gives a maximum mechanical, or true, strain of 121  $\mu\epsilon$  in tension and a minimum of 13  $\mu\epsilon$  in compression. These are well within the design constraints of 16,000  $\mu\epsilon$  for the GFRP bars. The corresponding stresses to the strains are, respectively 3.7 MPa and -0.4 MPa. These points correlate well with the field investigation on the first bridge deck reinforced with GFRP bars by El-Salakawy and Benmokrane (2007) with values of 62 and -125  $\mu\epsilon$  in the bars and concrete, respectively, with corresponding stresses of 2.60 and -3.56 MPa. With a known distance and recorded top and bottom strains, curvature is then calculated by:

$$\Phi = (\epsilon_{\text{top}} + \epsilon_{\text{bottom}}) / y \quad (1)$$

where  $\Phi$  = curvature in (1/inches) units;  $\epsilon_{\text{top}}$  = top strain gauge measured in  $\mu\epsilon$ ;  $\epsilon_{\text{bottom}}$  = bottom strain gauge measured in  $\mu\epsilon$ ;  $y$  = separation distance in (inches). These strains in the concrete are

within the limits of  $138 \mu\epsilon$  in tension at which concrete theoretically would crack and  $-3000 \mu\epsilon$  at which concrete fails in compression.

### 3.3.2 Linear Variable Displacement Transducers

The September 29, 2009 static tests are separated into three groups depending on the lanes being loaded. Using Truck “A”, Tests 1-3 were performed on the slow lane; using truck “B”, tests 4-6 were performed on the fast lane; both trucks “A” and “B” were used in tests 7-9 in their respective lanes. These measurements were made using LVDTs at the east and west diaphragms as shown in Figure 21. The 3 tests for each case were obtained by centering the rear axle of the truck over the east diaphragm, midspan, and west diaphragm, respectively; the deck deflections from the 2009 tests are shown in Figures 34-36. These deflections represent the maximum relative movement of the deck with respect to the prestressed girders, at the diaphragm locations.

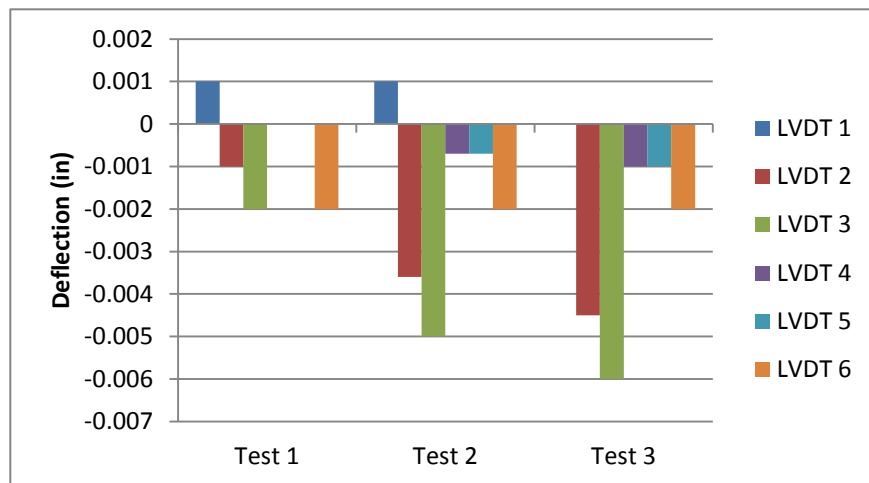


**Figure 34. Deck deflections from testing for Truck A, Sept. 29, 2009**

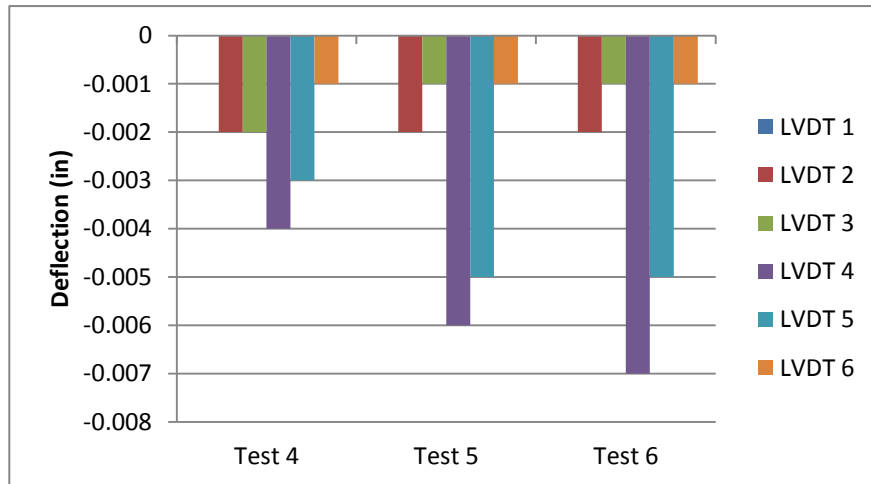


**Figure 35. Deck deflections from testing for Truck B, Sept. 29, 2009**

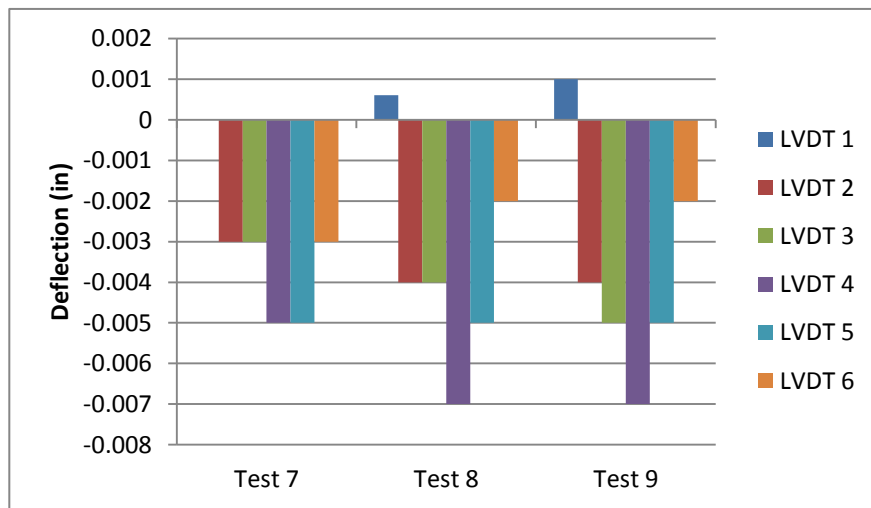


**Figure 36. Deck deflections from testing for Truck A and Truck B; Sept. 29, 2009**

From the September 29, 2009 tests, the highest relative deflections were found to be in the slow lane between girders 4 and 5 during Test 8 and Test 9, as shown in Figure 36; this is reasonable since both trucks “A” and “B” are located between midspan and the west diaphragm during Test 8 and are parked on the west diaphragm during Test 9. The magnitude of the relative deflection is very small, which shows that the bridge deck and girders have good composite

action. Mild post-tensioning in the longitudinal direction caused a maximum compressive strain in the panel of 164  $\mu$ strain which was not found to cause any difficulties in the performance of the panel.

The second truck load test was carried out on September 1, 2010. The truck weights for these tests are as follows: Truck “A” was 37.94 kips, Truck “B” was 45.68 kips. The deck deflections were very similar to results from the first truck load test with a maximum of 0.003 inches LVDT 3 and LVDT 4 are shown in Figure 37 for the case of both trucks “A” and “B” being on the bridge deck. Other LVDT’s read 0.001 inches or below.

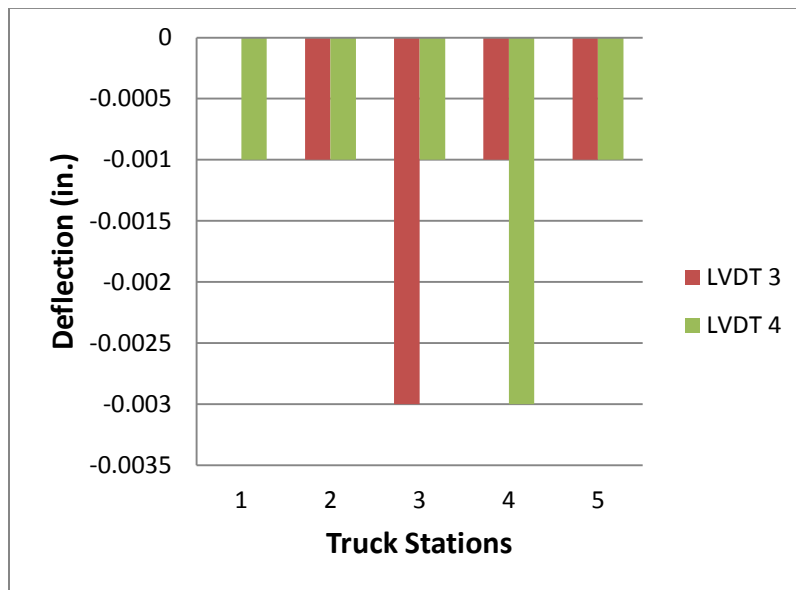


**Figure 37. Deck deflections from testing for Truck A and Truck B; Sept. 1, 2010**

Over the course of 2 years, the LVDT’s had recorded various maximum displacements, as shown in Table 6. The October 8, 2010 deflections of 0.15 inches and 0.14 inches exceed the

service load deflection limit of span/800 or 0.11 inches This exceeds the allowable due to an overloaded truck during construction time at a nearby location that month.

**Table 6. Deck deflections relative to girders (inches)**

	LVDT 2	LVDT 3	LVDT 4	LVDT 5
9/2009	0.003	0.004	0.006	0
5/2010	0.002	0.006	0.008	0.005
8/2010	0.014	0.004	0.005	0.015
9/2010	0.001	0.003	0.003	0.001
10/2010	0.15	0.14	0.017	0.027
11/2010	0.001	0.001	0.001	0.004
3/2011	0.001	0.002	0.002	0.003

Note: LVDT 2 is located between girders 2 and 3; LVDT 3 is located between girders 3 and 4

### 3.3.3 Girder Deflections

As expected, the maximum deflection of the girders occurred during Truck Load Test #8 on September 29, 2009 when both trucks were parked at the bridge midspan. The maximum deflection was 0.13 inches as shown in Figure 38, recorded in girder 4 located between the 2 trucks. The peak deflection recorded was 0.13 inches which is well below the AASHTO limit of  $L/800$ , or in this case 1.32 inches All girder deflections were measured with survey equipment; the uplift in girder 6 is due to operational human error while collecting survey data.

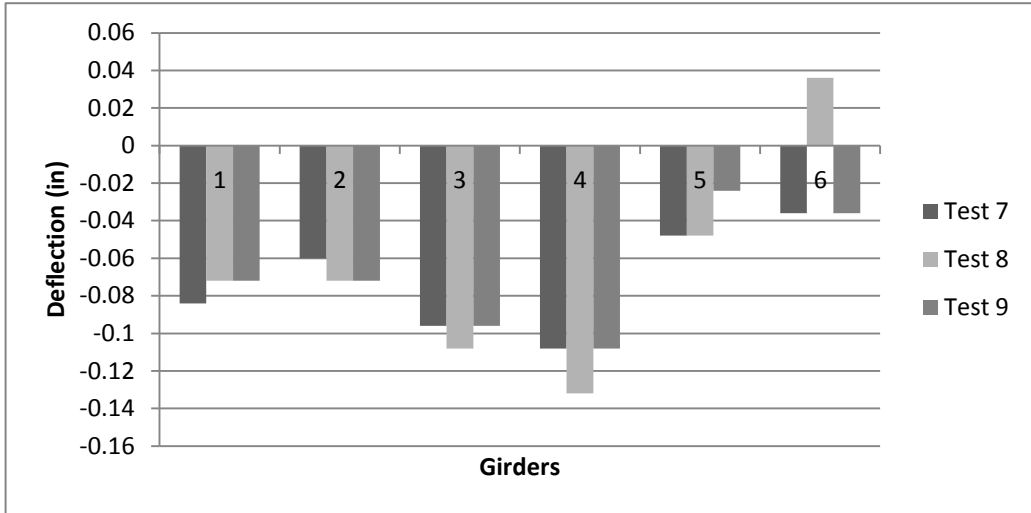


**Figure 38. Midspan girder deflections for tests 7 through 9 for Girder #4**

During truck load test 9, additional girder displacements were measured above the west diaphragm. This was done to correlate girder deflections and panel deflections at the same point. Additional deflection data was taken for girders 2 and 3, as shown in Figure 39. The deflection of the diaphragm is assumed to be linear between the girders. The displacement of the diaphragm at midspan between girders 2 and 3 was calculated to be 0.06 inches. Combining this with the panel deflection from LVDT #2 for the same test, the total deflection of the panel located above LVDT #2 has been calculated to be 0.064 inches. The relative deflection of the panel with respect to the least deflected girder can be determined using half the difference between the 2 girders and deflection data from LVDT #2. This results in a deflection of 0.016 inches relative to girder 3. Both of these values are below the AASHTO limit of 0.101 inches.

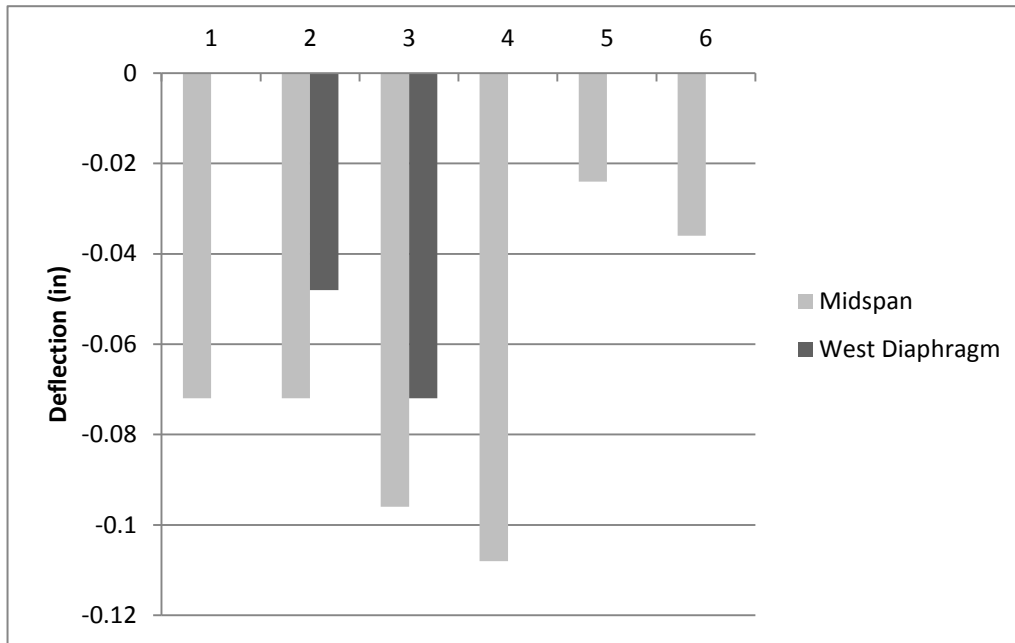


**Figure 39. Girder deflections for truck load test 9**

### 3.3.4 Accelerometers

Dynamic truck load tests were also performed on September 29, 2009 before the bridge opened to traffic and consisted of 5 tests. The 6 accelerometers are attached to the bottom of the flanges at midspan of the girders, as shown in Figure 21; all 6 accelerometers measured data as shown in Figure 40. Accelerations measured at the midspan of the prestressed girders for the 43.16 kips “B” truck traveling in the fast lane at 40 mph, showed that the maximum vertical acceleration recorded during this test was 0.015g (Test 1 in Figure 41). By comparison, the maximum acceleration for the case of 65 mph recorded was 0.026g in girder 2 (Test 2 in Figure 42).

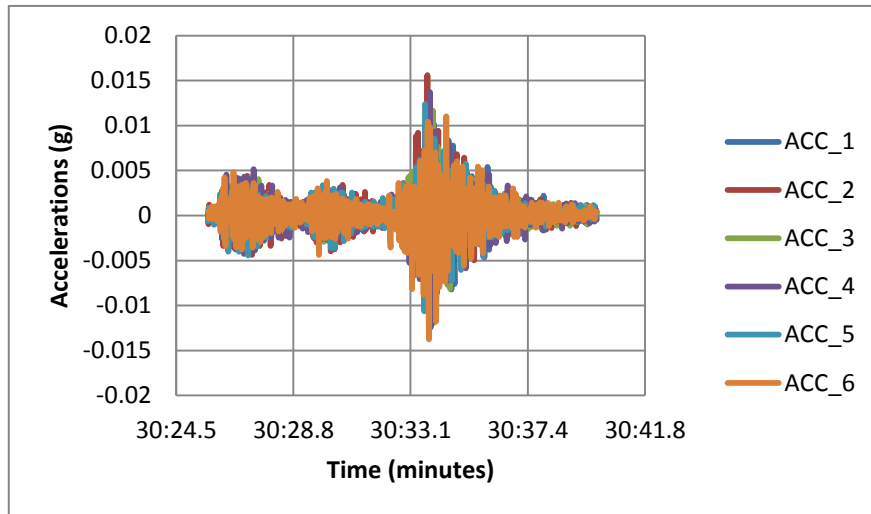


**Figure 40. Acceleration record for truck B traveling at 40 mph for Test 1**

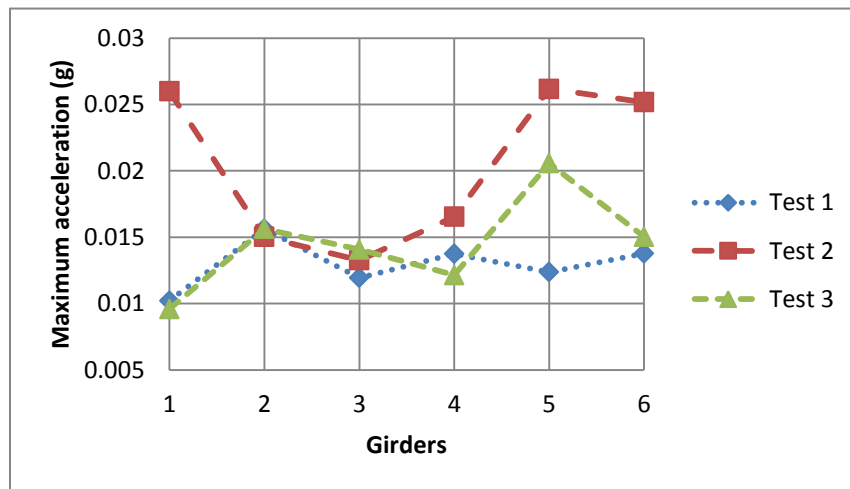


**Figure 41. Maximum accelerations for Truck B traveling at 40 mph**

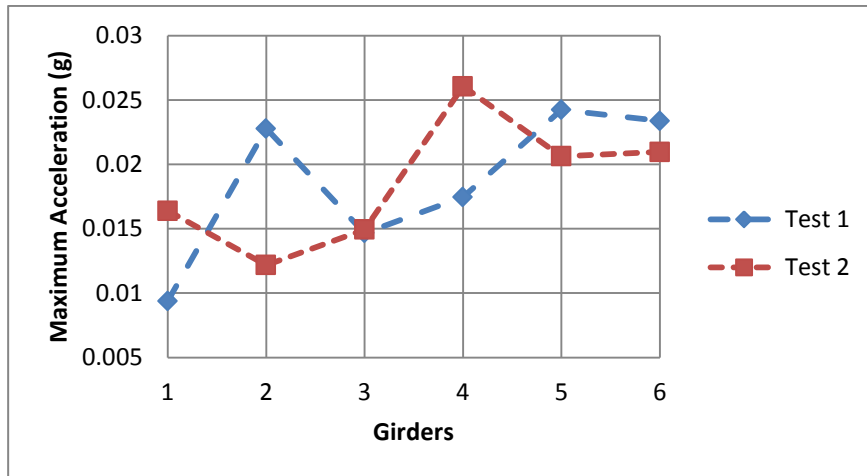


**Figure 42. Maximum accelerations for Truck B traveling at 65 mph**

Dynamic truck load tests carried out during the second truck load test of September 1, 2010 with trucks weights “A” of 37.94 kips and “B” of 45.68 kips showed that the maximum overall vertical acceleration recorded during this test was 0.014 g, as shown in Figure 43.

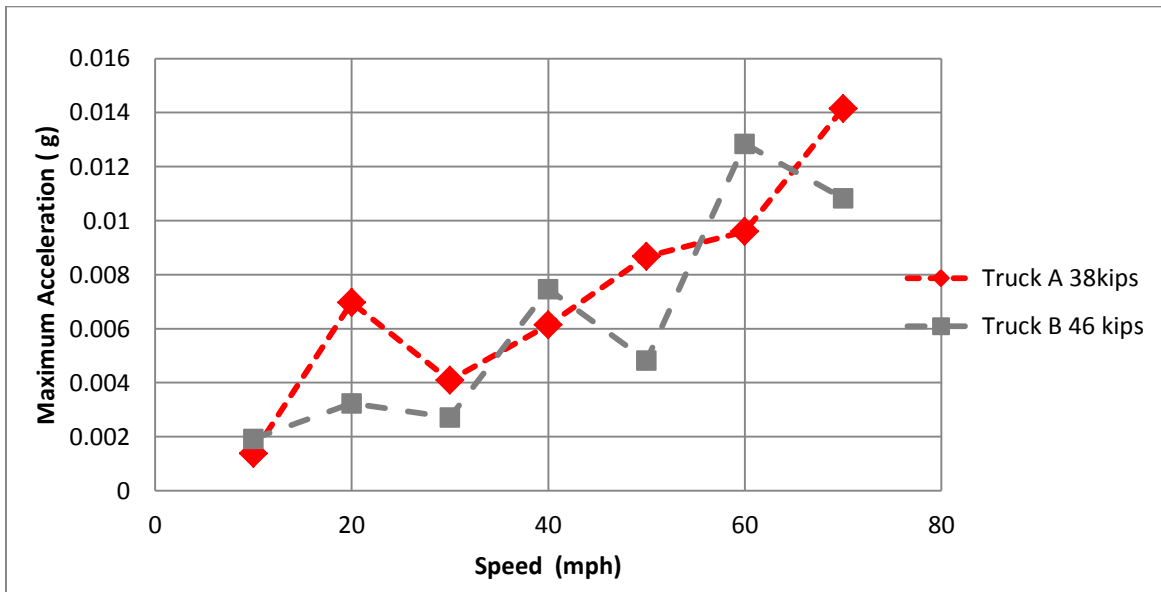


**Figure 43. Maximum accelerations from second truck load test performed Sept. 1, 2010, as a function of truck speed**

A third dynamic truck load test was performed November 19, 2010 with a truck weighing 65.9 kips. The truck was positioned in the slow lane and, due to the heavy weight of the truck, could only reach a maximum speed of 55 mph. The maximum acceleration was 0.016 g at 50 mph as shown in Figure 44.

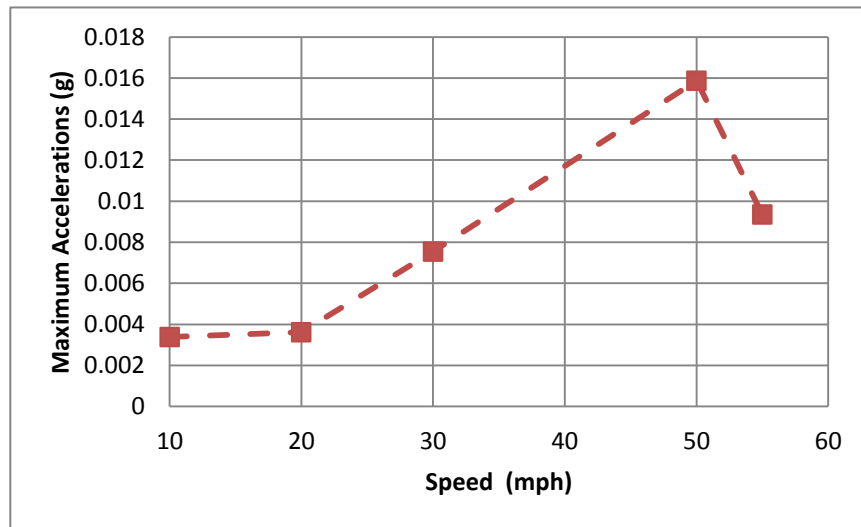


**Figure 44. Maximum acceleration from third truck load test performed Nov. 19, 2010, as a function of truck speed**

Truck load tests were carried out in a controlled environment, in which the weather conditions were good, and the weight and speed of the truck were known. However, some of the higher acceleration data measured from long term monitoring comes from continuous monitoring and capturing “snapshots” of real life conditions at the bridge. The data and picture below in Figures 45-46 are a representation of such events.

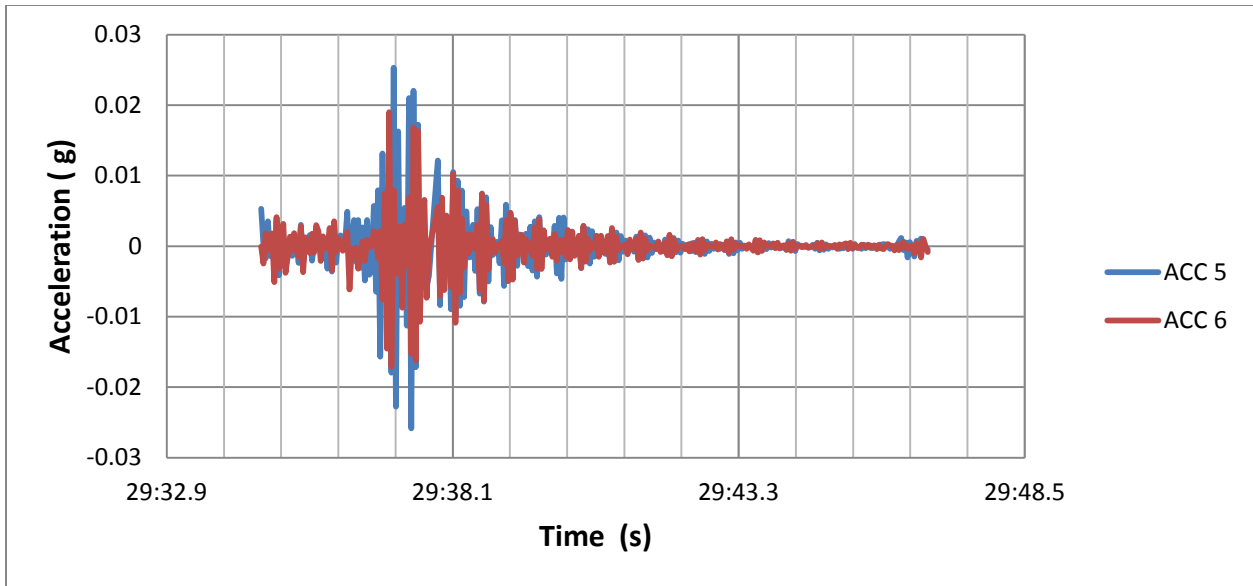


**Figure 45. Acceleration record of Oct. 22, 2010 during a construction period**



**Figure 46. Image for acceleration record of Oct. 22, 2010 during a construction period**

The particular flatbed truck in Figure 46 gave a maximum acceleration of 0.025 g as shown in Figure 45. The weight and speed of the truck are not known. However, the traffic

camera shows construction that month and the LVDTs recorded high relative deck deflections up to 0.15 inches that month as well.

In addition to special events and planned testing, real time accelerations are captured on screen. These responses are significantly larger than what was observed with controlled annual truck testing and are analyzed; these trucks represent what traffic actually is on the bridge daily. Over the course of three days, representative screen shots were captured; the highest daily response is shown in Figures 47-49.

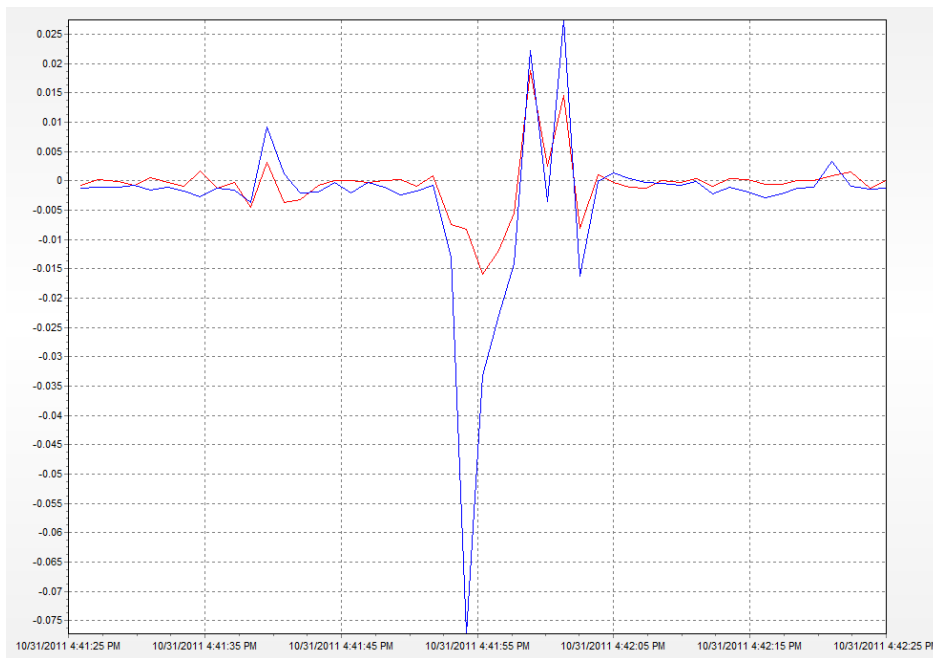


**Figure 47. Acceleration of 0.075 g at girder 2 on October 31, 2011**

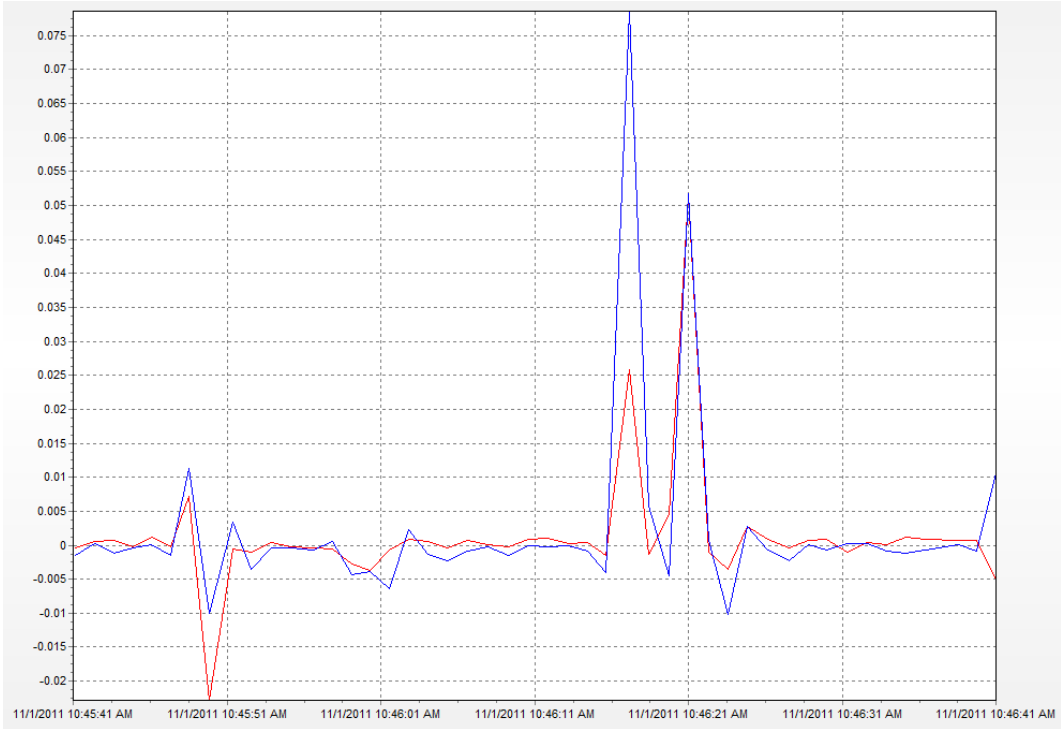


**Figure 48. Acceleration of 0.078 g at girder 2 on November 1, 2011**

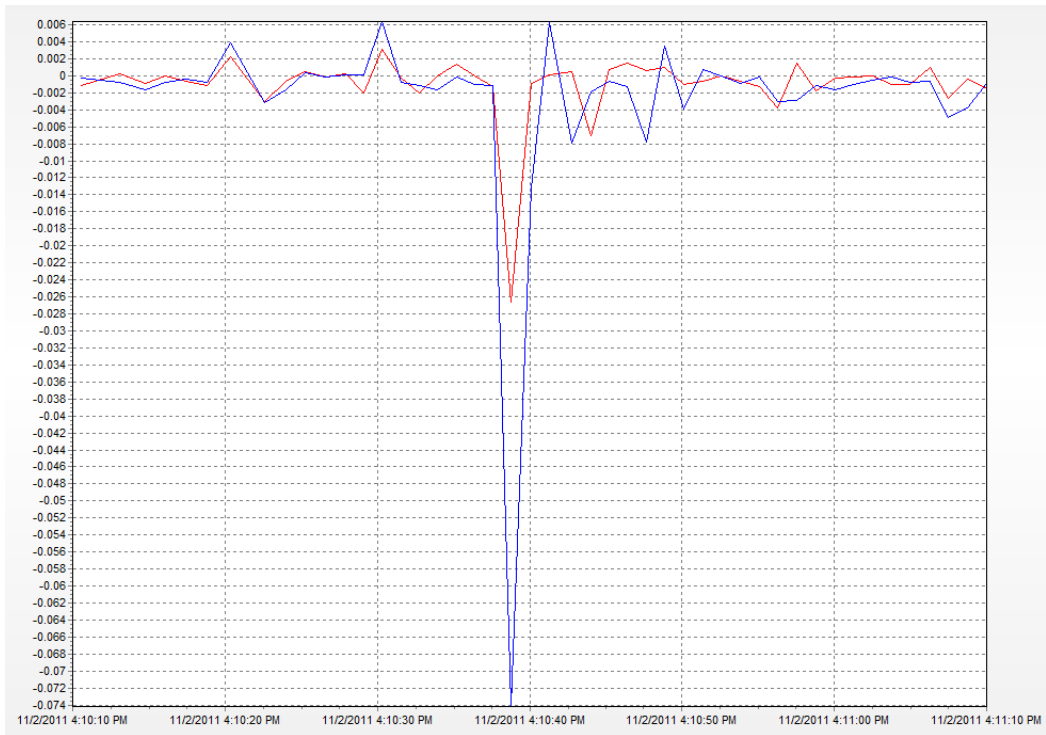


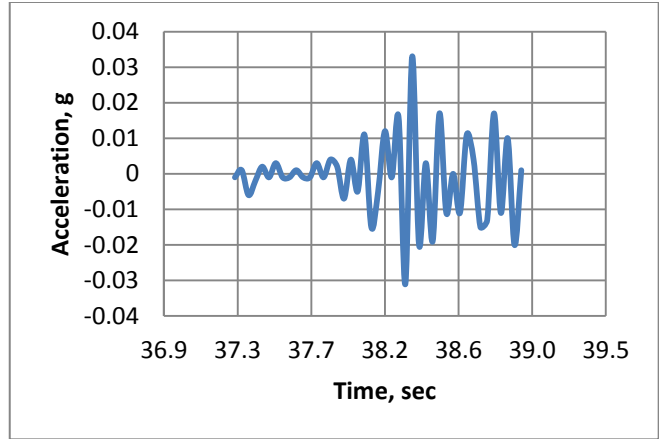
**Figure 49. Acceleration of 0.074 g at girder 2 on November 2, 2011**

As observed in Figures 47-49, ambient data show accelerations without knowledge of the truck weight or speed. On November 21, 2011 a fourth truck load test was carried out. UDOT Peerless Port of Entry 8037 No. Highway 6 weighed a continuous sample of 90 trucks. The port of entry is approximately 10 miles from the bridge. The research team collected the speed of each truck using a Pro Laser III LiDAR gun while the truck was over the bridge. Thus, both truck weight and speed are known. The sample set included trailers, tankers, flatbeds, cab, and small trucks. The times were taken as the trucks passed over the bridge, making it possible to match up the truck with the accelerometer data recorded. Pictures and signals are shown below in Figure 50.



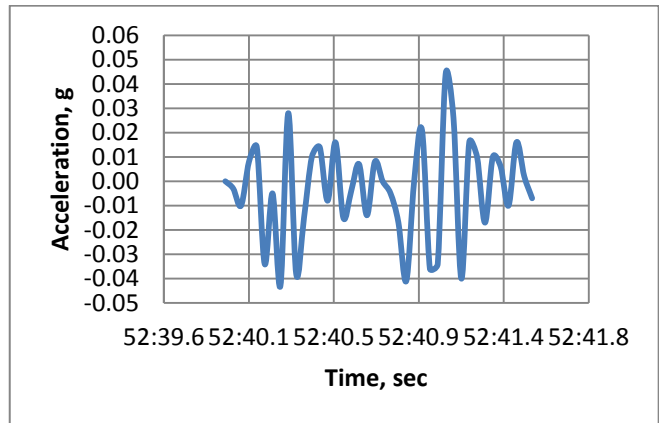
**Truck weight = 60.98 kips,**

**Truck speed = 48 mph**



**Truck weight = 119.22 kips,**

**Truck speed = 62 mph**



**Flatbeds are not weighed**

**Truck speed = 67 mph**

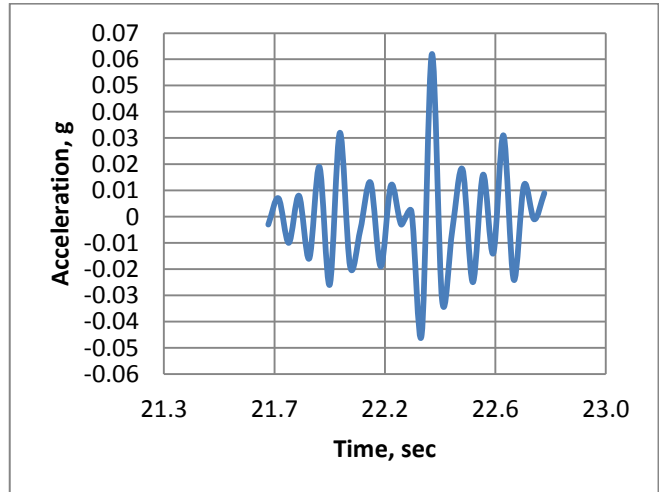


**Figure 50. Sample of trucks in the data set and their corresponding acceleration response**

Of the data set, 19 trucks were able to be matched with a speed, weight, and acceleration signal and are shown in Figure 51 below. It should be noted that the acceleration response is grouped in the following ranges: 0 to 5%g, 5% to 7.5%g, and 7.5% to 10%g. The maximum acceleration was 0.105g from a flatbed truck that was hauling a load marked “oversized load” that weighed 62.14 kips and was traveling at a speed of 65 mph.

The heaviest truck was 119.22 kips travelling at 62 mph; the corresponding response was 0.057g. The fastest truck tested was travelling at 68 mph and weighed 60 kips; the corresponding response was 0.0529g. As mentioned earlier, the largest response was 0.105g and was triggered by a 62.14 kips truck traveling at 65 mph; however, there was another truck on the bridge at the same time.

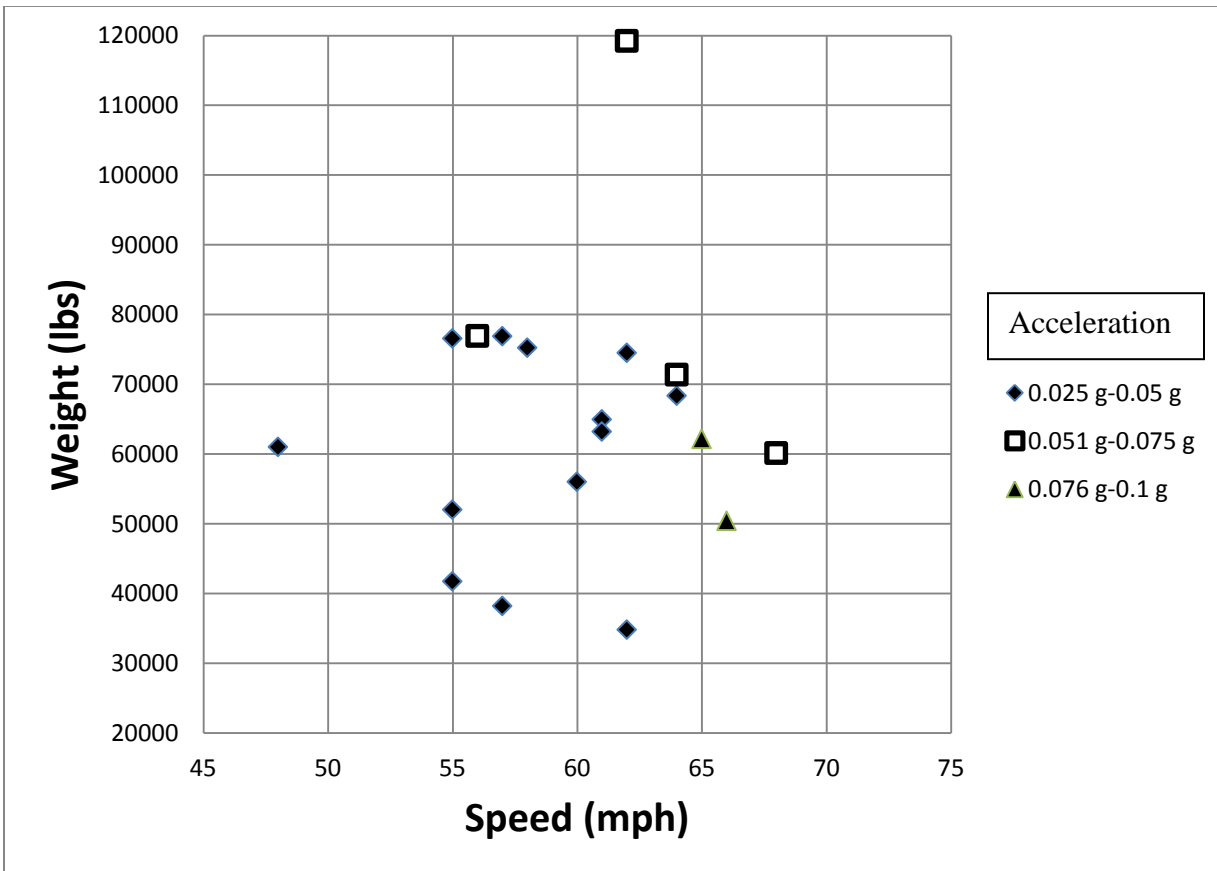


Figure 51. Acceleration as a function of weight and speed from Nov. 21, 2011 test

THIS PAGE LEFT INTENTIONALLY BLANK

## 4.0 ANALYTICAL RESULTS

### 4.1 Lifting Curvature Diagram

From the recorded strains during lifting, the curvature of the panel was determined using Eq (2), where “ $\epsilon$ ” is the strain recorded and “ $d$ ” is the distance between the top and bottom reinforcement mats. The measured curvature diagram from the first lift of P2-05 is shown in Figure 52, along with 2 arrows representing the closest lifting points. The theoretical curvature from PCI will be compared to the measured curvature at 3 points, under each lifting point, and at midspan between the 2 lifting points.

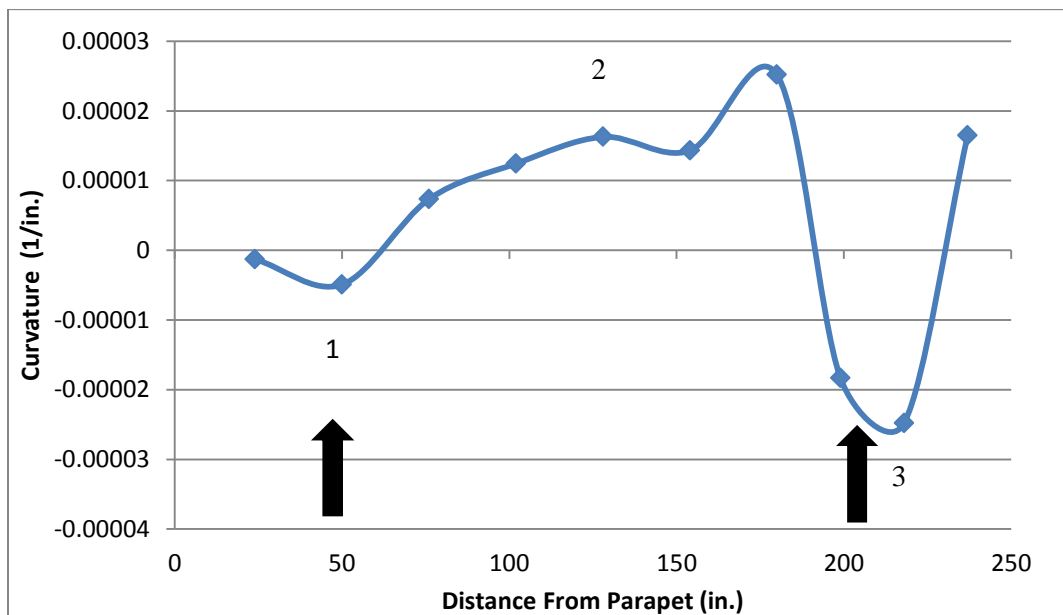


**Figure 52. Curvature diagram from experimental results (arrows represent lifting points)**

The measured curvature can be obtained as:

$$\varphi_{measured} = \frac{\epsilon_{top} - \epsilon_{bottom}}{d} \quad (2)$$

The curvature under the first lifting points is  $4.9 \times 10^{-6}$  /inches and is within the range of theoretical curvatures. At the midpoint between to 2 lifting points the curvature is  $1.63 \times 10^{-5}$  /inches which is 1.6 times the upper limit of PCI's theoretical range. The curvature under the second lifting point is  $2.5 \times 10^{-5}$  /inches and is 2.7 times the upper bound of PCI's theoretical curvature. The difference between the theoretical and measured curvature is thought to come from fixed end moments induced by uneven lifting, as well as cable deformations. The panel was lifted at 4 points and underwent uneven deformation due to different vertical forces in the cables. The different vertical forces strained the lifting cables differently, creating a scenario similar to that found when a multi span beam undergoes uneven settlement at its supports, thus creating fixed end moments at each support.

## 4.2 Post-Tensioning

The post-tensioning cables were each tensioned with a force of 40.8 kips. The total jacking force from all the strands in the west bound bridge was found to be 1346 kips. From the initial jacking force of the post-tensioning strands, the stress in the slab was calculated by dividing by the cross-sectional area of the panel, and was found to be 295 psi. Using the modulus of elasticity of concrete, the theoretical change in strain of the concrete was found to be  $62 \mu\epsilon$ , as shown in Eq (3):

$$\frac{\text{Total Jacking Force}}{(\text{Cross Section Area}) \cdot (E_c)} = \frac{\frac{40.8 \text{ kips} \cdot 3 \text{ strands}}{\text{strand}} \cdot 11 \text{ pockets}}{(4572 \text{ in}^2) \cdot (4.675 \cdot 10^6 \text{ psi})} = 62 \mu\epsilon \quad (3)$$

This microstrain is approximately half the average of 130  $\mu$  strain recorded by the VWSGs. However, the recorded values also take into account other strains such as creep and shrinkage.

### 4.3 Panel Deflections

During the design of the bridge, the deflection of the panel relative to the girders was calculated using the HL-93 truck load and the deflection equation from ACI 440.1R-06 (Eq 4). The deflection of the deck relative to the girders due to positive live load moment was calculated as 0.10 inches (Nix 2010). The maximum deflection of the panels relative to the girders recorded during the truck load test was 0.007 inches, much less than the calculated deflection. Furthermore, the peak deflection of 0.007 inches was well below the AASHTO limit of L/800 or in this case 0.101 inches. Taking into consideration that the truck load test involved lighter trucks, the deflections are small enough to suggest that the changes made to the design of the bridge were successful in maintaining small service deflections.

$$(\Delta_i)_{LL} = \frac{5 * M_{LL} * l_{eff}^2}{48 * E_c * (I_e)_{LL}} = \frac{5 * (5.56 \text{ kip ft}) * (83 \text{ in})^2}{48 * (3.834 * 10^3 \text{ Ksi}) * 123.223 \text{ in}^4} = 0.101 \text{ inches.} \quad (4)$$

However, during long-term monitoring, panel deflections as high as 0.15 inches were observed during construction periods, as shown in Table 6.

### 4.4 Girder Deflections

The maximum deflection of the girders was 0.13 inches and it occurred during truck load test 8. This was well below the AASHTO limit of 1.325 inches. During truck load test 8, the trucks were positioned primarily over girders 3-5; however girders 1 and 2 each deflected 0.07

inches, and girder 6 deflected upward 0.03 inches. The small deflections observed across girders 1 -5, and the positive deflection observed in girder 6, provides additional evidence that panel-girder continuity was achieved via the blockouts. Moreover, the panels were successful in transferring live loads evenly among the girders.

#### 4.5 Accelerometers

From the collected data, the impact factor and damping coefficients were evaluated. The first truck load test accelerations shown in Figure 53 are used in order to compare with the static deflections of the girders before the bridge opened to traffic.

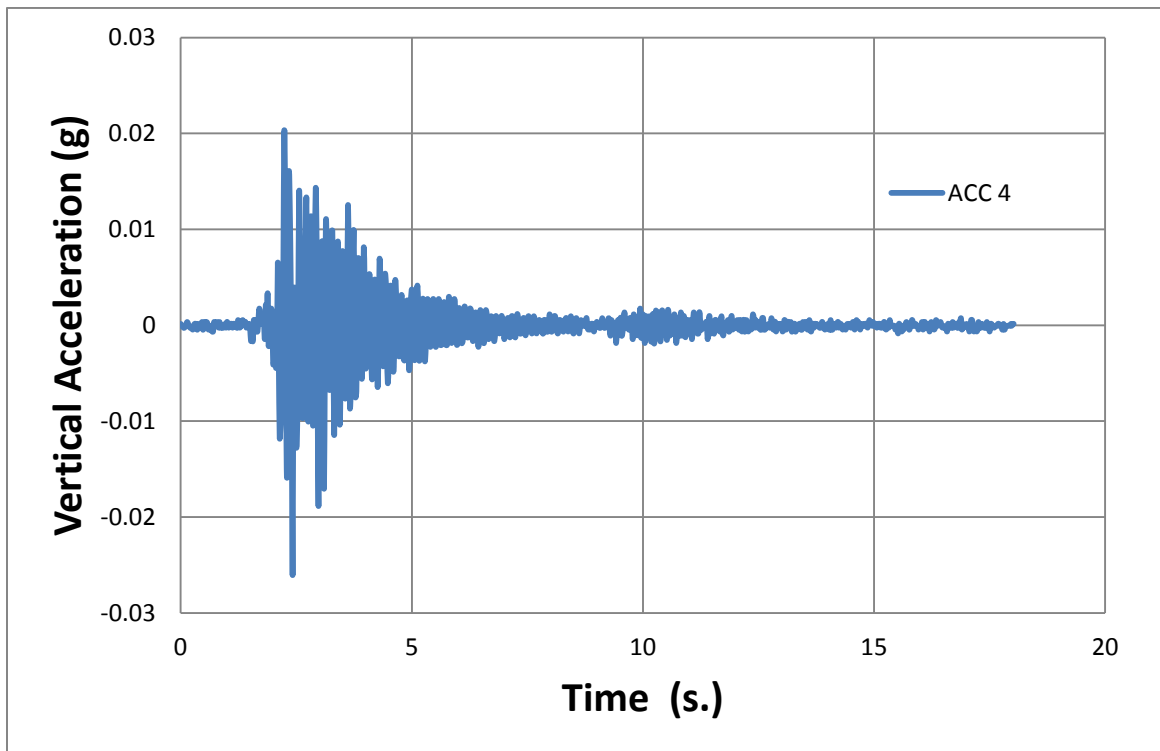


**Figure 53. Acceleration data from first truck load test, September 2009**



### **Figure 54. Dynamic Deflection of 43 kip truck at 65 mph over girder 4**

To find the impact factor, the dynamic displacement is divided by the static displacement. The static displacement on girder 4 for truck B during the September 2009 test was 0.096 inches, giving an impact factor of 1.15. This number represents one test and one data point; however, a similar truck from ambient data weighing 42 kips and travelling at 60 mph was analyzed and gave an impact factor of 1.20. This shows good correlation and is within the AASHTO code limit.

## **4.6 Modeling**

### **4.6.1 Bridge Finite Element**

SAP 2000 was used to generate finite element models of the bridge. The deck, girders, abutment springs and prestressed tendons were included in the model as shown in Figure 55. Area elements were used for the deck and girders, line elements for the prestressed tendons in the girders and spring elements for the abutments. The abutments were modeled as a fixed-fixed integral abutment condition with rotational springs.

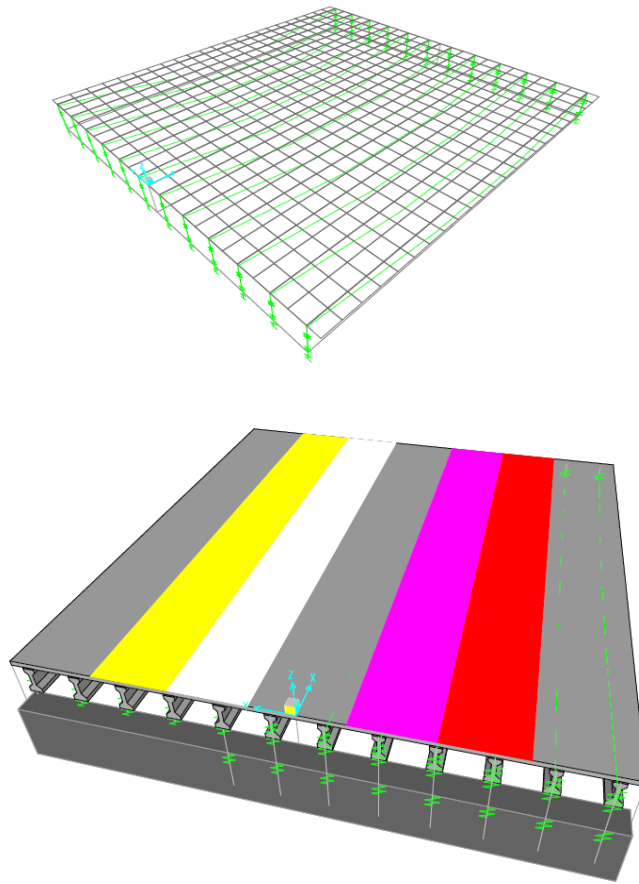


**Figure 55. Model showing lanes, girders and abutments**

The accelerometers in the west-bound “fast” lane gave the highest response; therefore, that lane in Figure 56 was modeled and truck traffic loads were applied. The model consisted of area elements that were analyzed by a time history loading to capture the dynamic loading on the bridge. The AASHTO 2009 design code was used to check the allowable moment and shear in the girders and structure as a whole.

Dead load, prestress load, and a dynamic truck load using a 44 kip truck going 65 mph were used for the analysis. The maximum deflections for the 3 loads were -0.201 inches,  $+3.03 \times 10^{-4}$  inches, and -0.003 inches respectively, which are shown in Figures 56-58.

Using an AASHTO Service I case load combination, the bridge was analyzed with all 3 loads applied. This gave a maximum displacement of -0.203 inches as shown in Figure 59 which is still within the span/800 design limit.

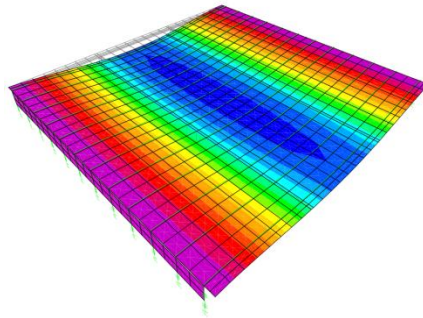


**Figure 56. Finite Element model of the dead loads; maximum deflection is -0.201 inches**

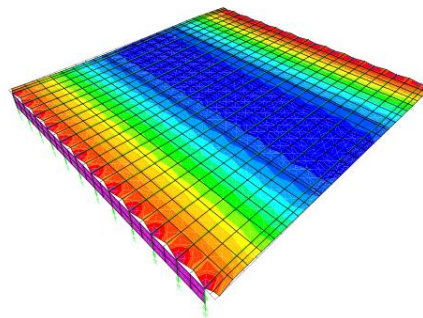


**Figure 57. Finite Element model of the prestress loads; maximum deflection is +0.0003 inches**

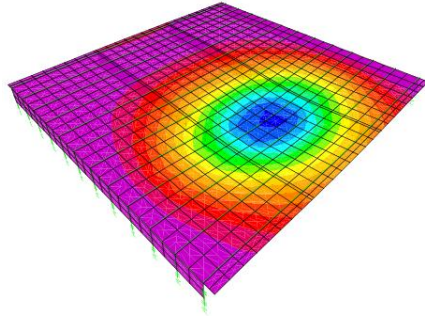


**Figure 58. Finite Element model of the truck loads at midspan in the inside lane; maximum deflection is -0.003 inches**

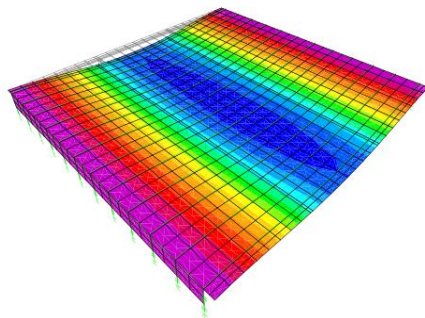


**Figure 59. Total bridge deflection of -0.203 inches under AASHTO LRFD Service I load case combination**

12 bridge modes were included and the 2 most significant ones (Mode 1 and Mode 2) are shown below in Figures 60 and 61. The period for Mode 1 is 0.146 s.; the period for Mode 2 is 0.140 s. It is important to note that mode 1 is the mode shape for the fundamental period of 0.146 s. This period is close to the period measured during the first truck load test, which was approximately 0.12 s, as shown in Figure 54.

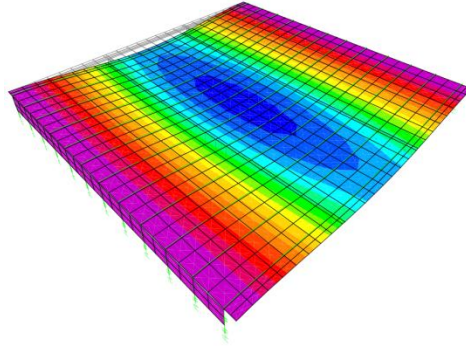


**Figure 60. Mode 1, period of 0.146 s**

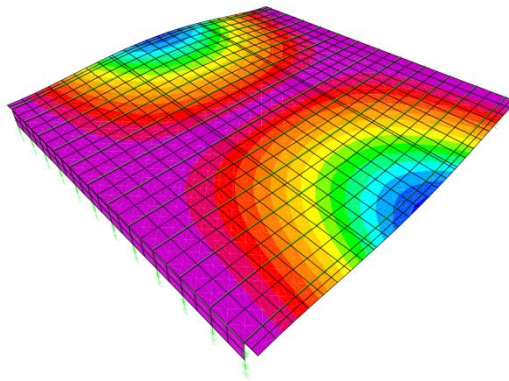


**Figure 61. Mode 2, period of 0.140 s**

The bridge was also analyzed for stress, as shown in Figure 62, to compare strain data. The maximum stress was 913 psi (tension) and the minimum was -393 psi (compression). Dividing by the elastic modulus of the concrete, 4506 ksi, gives a strain of 203  $\mu\epsilon$  (tension) and -87  $\mu\epsilon$  (compression).

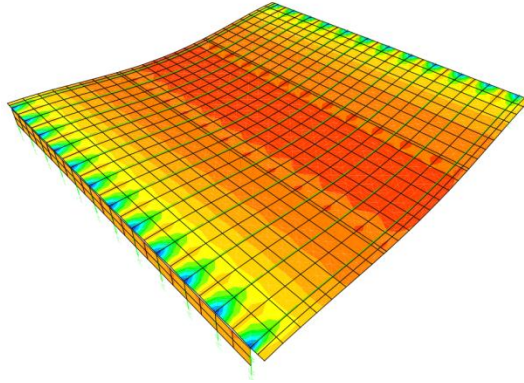


**Figure 62. Stress on bridge deck with a maximum of 913 psi and a minimum of -393 psi**

A static model of 2 trucks, 1 in each lane, parked at midspan was analyzed as shown in Figure 63. The truck live load case gives a deflection of 0.003 inches; the total bridge deflection including dead load and prestressing was 0.17 inches. This compares well with the maximum total static measured deflection of 0.13 inches in the girders shown in Figure 38, and is well within the allowable limit of span/800 or 1.32 inches. A comparison of experimental data with modeled data is shown in Table 7.

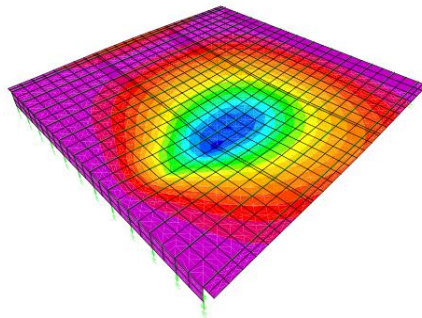


**Figure 63. Static truck load at midspan in inside lane; deflection of -0.003 inches**

**Table 7. Comparison of collected data to computer generated model**

	Model	Collected Data
Maximum Strain	207 $\mu\epsilon$ (tension)	121 $\mu\epsilon$ (tension)
Minimum Strain	89 $\mu\epsilon$ (compression)	13 $\mu\epsilon$ (compression)
Maximum Static Bridge Deflection	-0.203 inches	-0.13 inches
Deck Deflections Due To Trucks	-0.003 inches	-0.007 inches

#### **4.6.2 Deck Panel Lifting Strains**

The 2 panel lifts, shown in Figure 10 marked Lift 1 and Lift 2, were modeled using finite elements. The recorded deflection of the panel on the ground supported by 4 HSS pipes was 0.002 inches as shown in Figures 64 and 65. The recorded stress and strain of the panel on the ground supported by 4 HSS pipes were 96 psi and 21  $\mu\epsilon$  (tension) as shown in Figures 66 and 67. Strains were modeled at the top surface of the concrete. However, the gauges measuring the strain data were located on the GFRP bars, 1.5 inches below the surface of the panels. Therefore, a more accurate strain of 14  $\mu\epsilon$  (tension) is shown at the gauges in Figure 67.

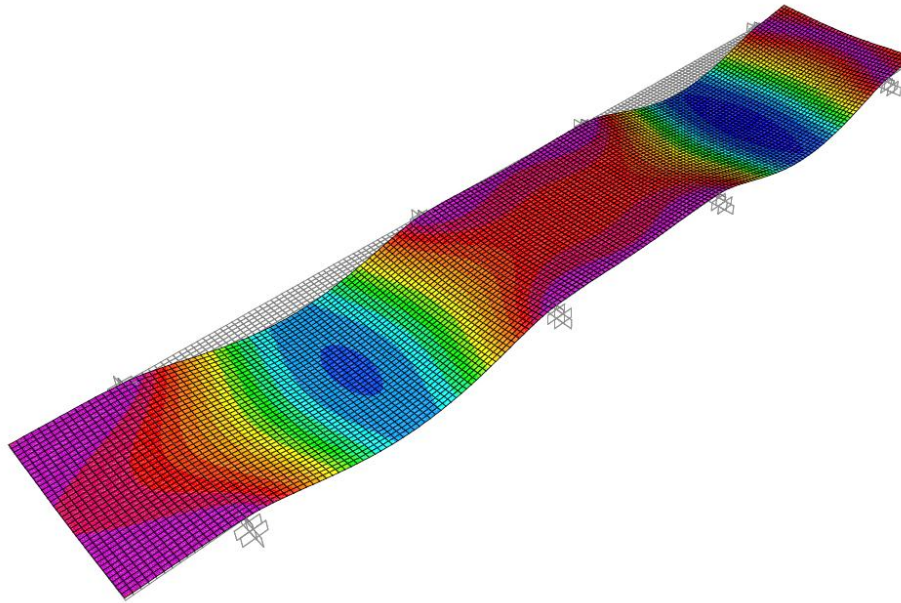


**Figure 64. Deflected panel with a maximum deflection of 0.002 inches**

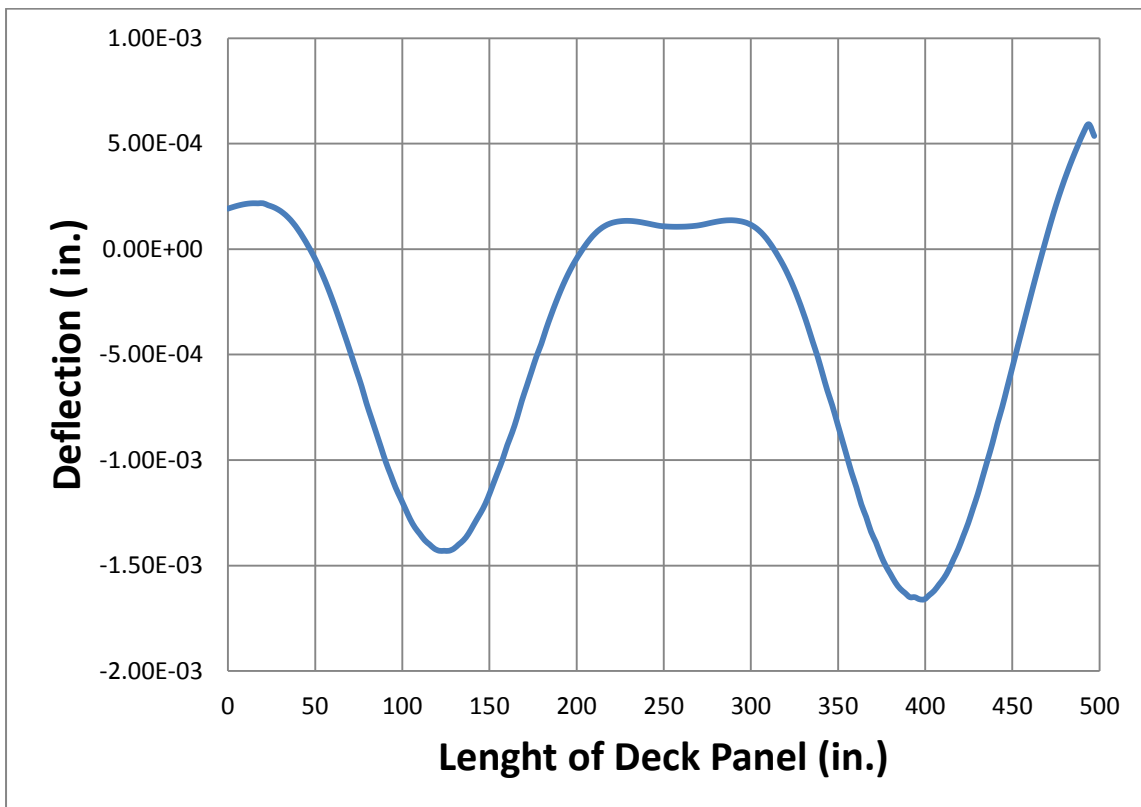


**Figure 65. Midline deflection for panel sitting on the ground**

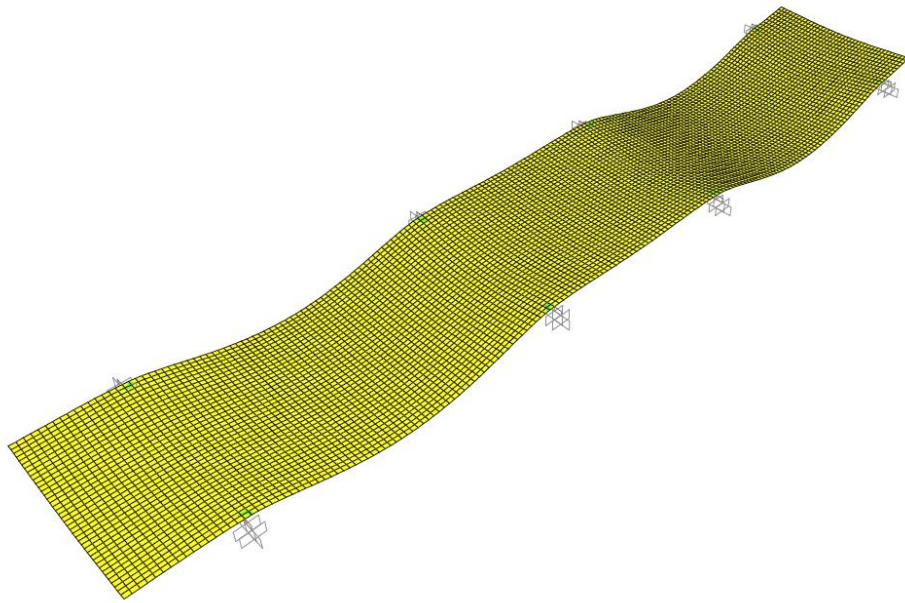


**Figure 66. Maximum stress of 96 psi in the panel and 160 psi at supports**

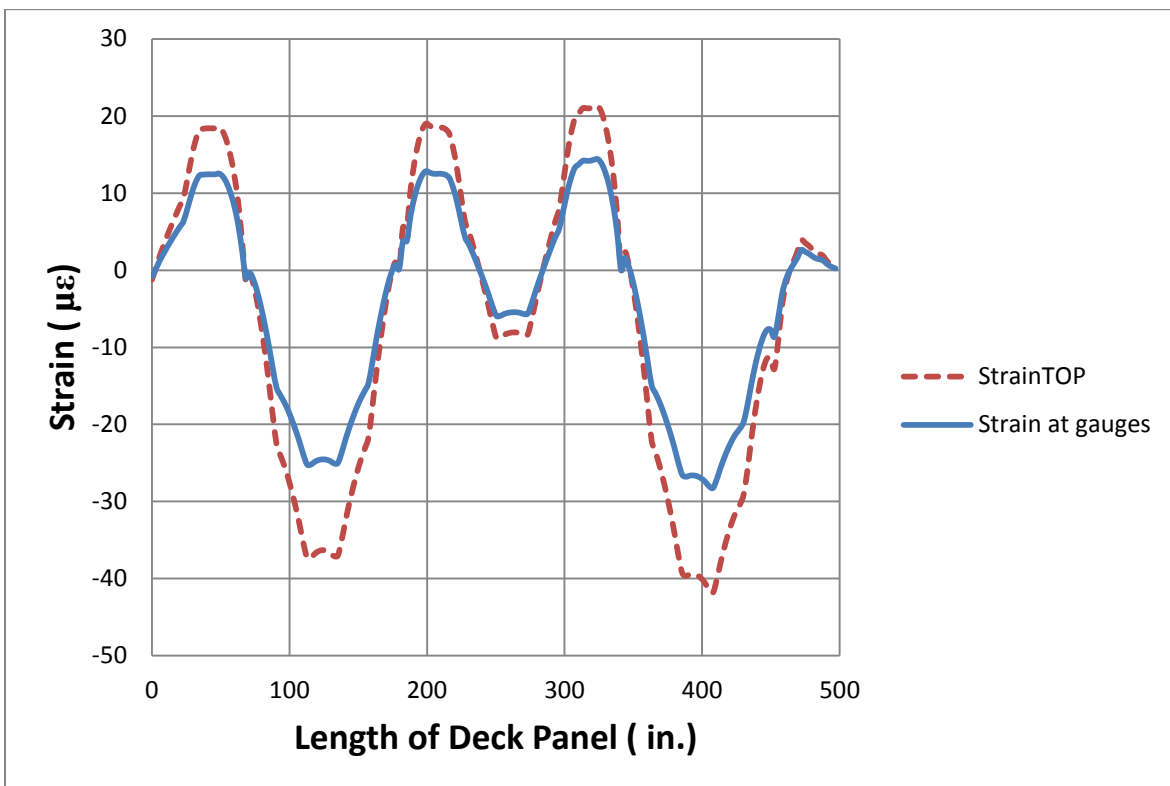


**Figure 67. Mid-line strains in panel while on ground**

The second lift was modeled without the parapet. The maximum stress on the top of the slab while in air was 100 psi with a corresponding strain of  $-22 \mu\epsilon$  shown in Figures 68 and 69. The maximum deflection in air was 0.026 inches, shown in Figures 70 and 71.

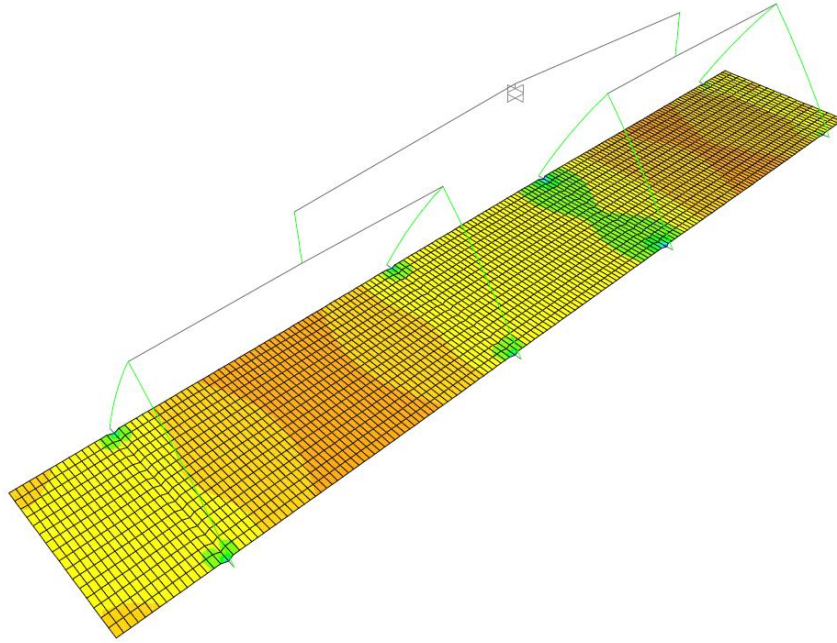


**Figure 68. Maximum stress of 100 psi at the top of deck panel while lifting**

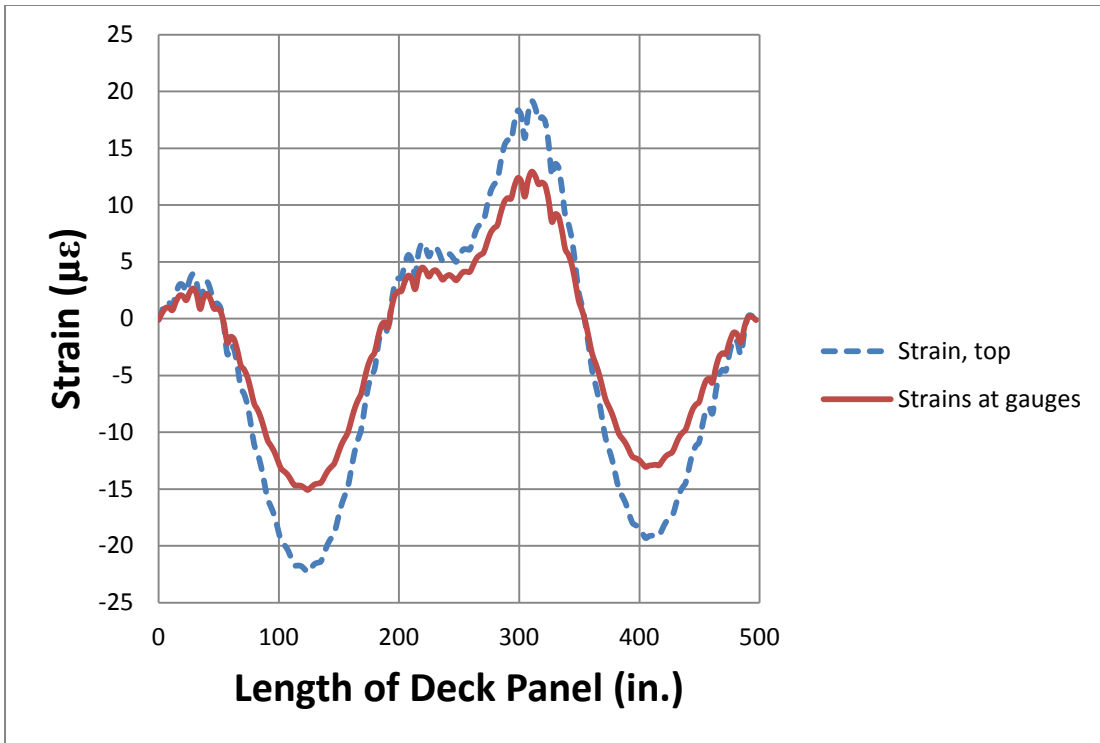


**Figure 69. Mid-line strain without parapet**

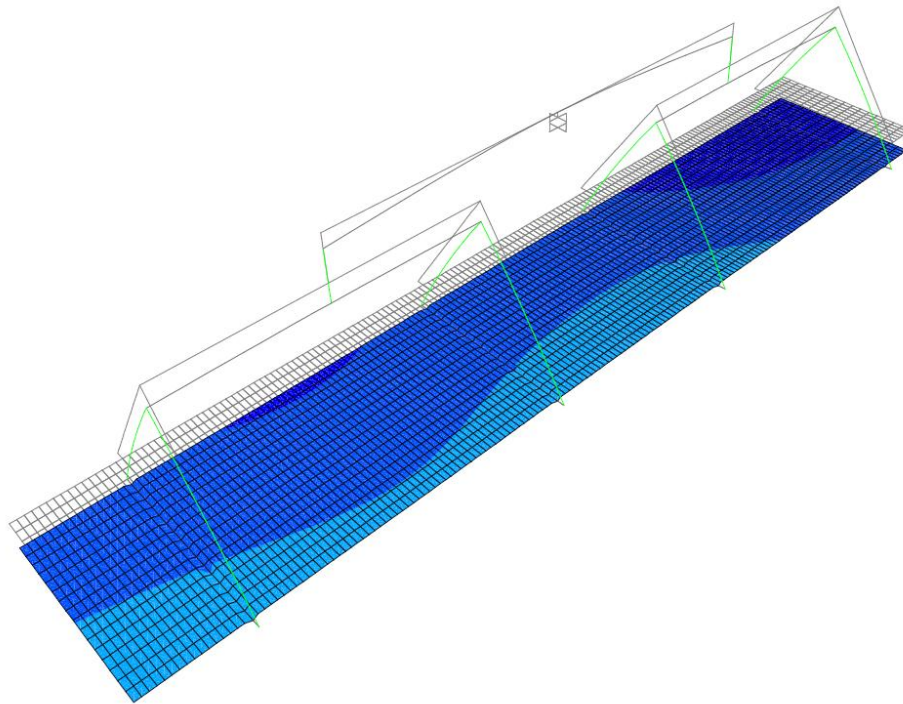


**Figure 70. Deflected panel with a maximum midline deflection of 0.026 inches**

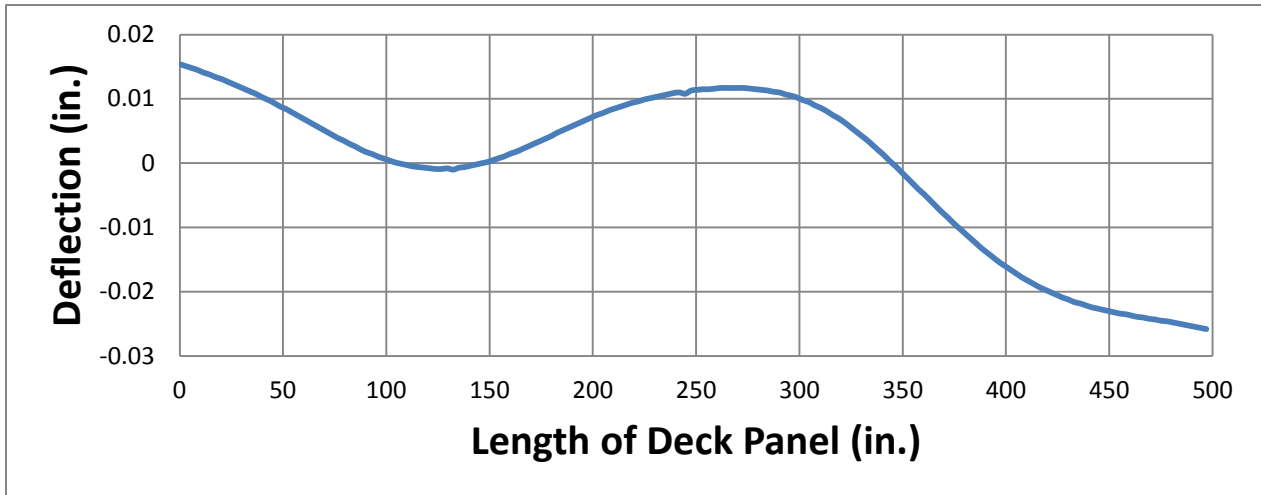


**Figure 71. Midline deflection for panel lifting without the parapet**

The third lift was modeled with the parapet on the left side of the panel. The parapet was modeled as an equivalent distributed load placed at the end of the panel. The maximum deflection in the air was 0.34 inches as shown in Figures 72 and 73. The maximum stress on the top of the slab while in the air was 276 psi with a corresponding midline strain of  $59 \mu\epsilon$  shown in Figures 74 and 75. These values correspond well with recorded top strain and are close to the experimentally observed strains in the panel. The calculated deflections are small but reasonably close compared to the predicted deflections (Nix 2010).

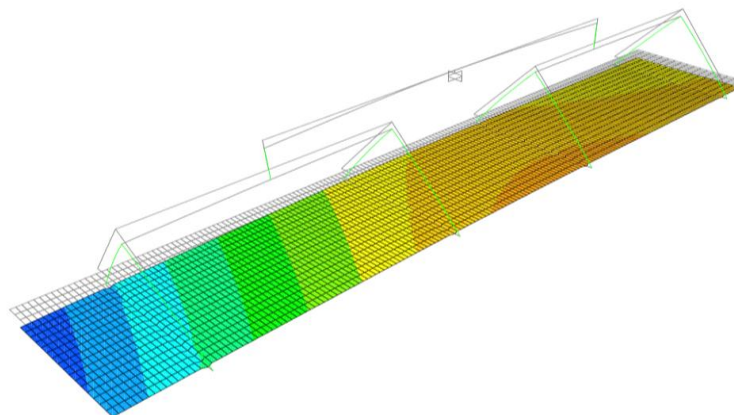


**Figure 72. Deflected panel with a maximum midline deflection of 0.34 inches**

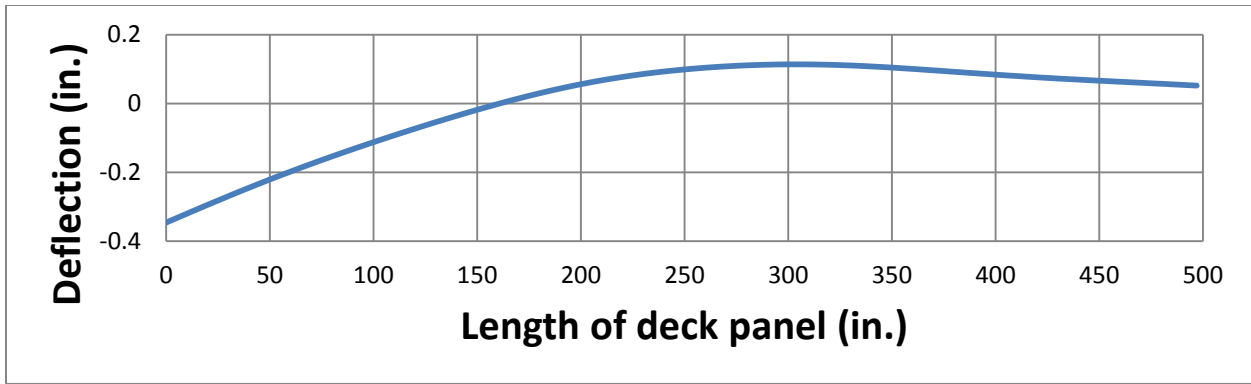


**Figure 73. Midline deflection for panel lifting with the parapet**

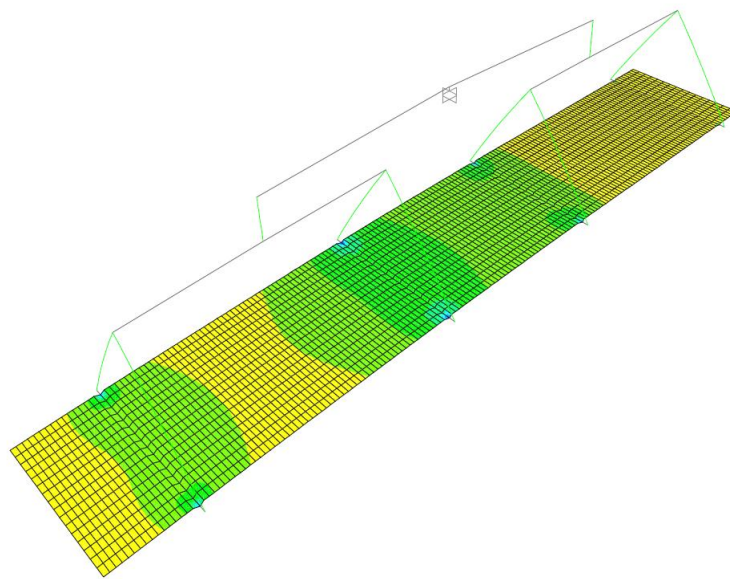


**Figure 74. Stress of panel with parapet while lifting is 276 psi max**

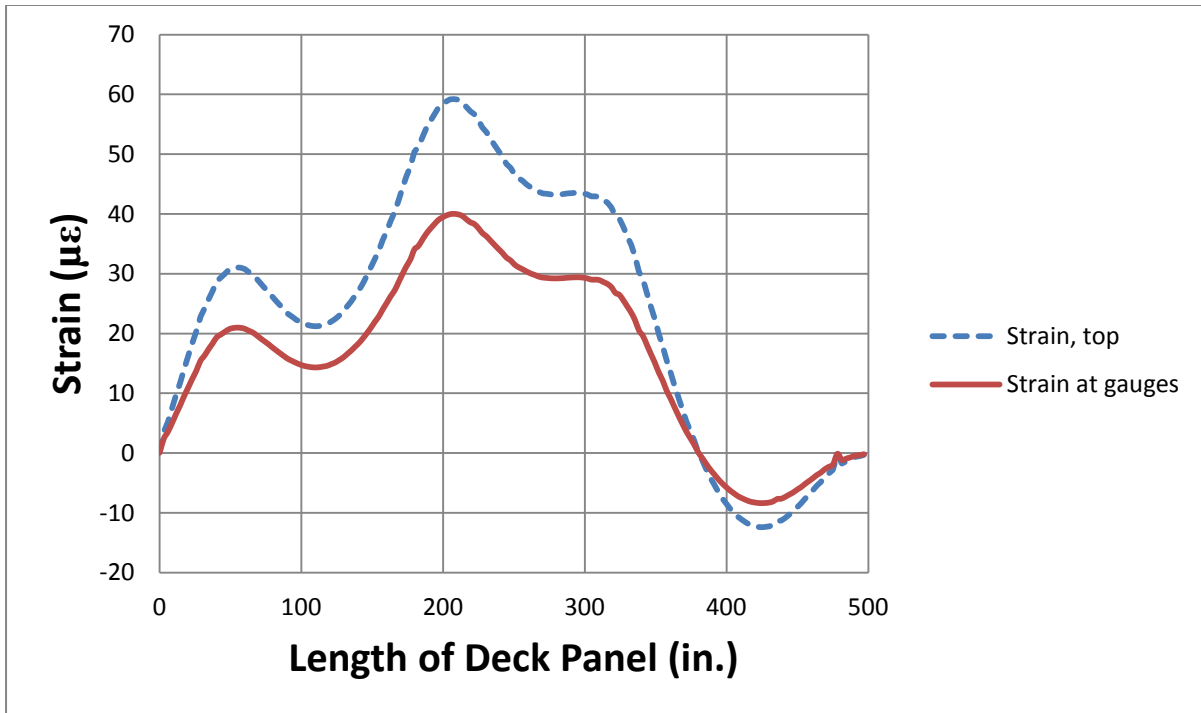


**Figure 75. Mid-line strain with parapet**

#### 4.7 Cost Analysis

The cost differential of new materials is of the utmost importance. Cost data from the Beaver Creek Bridge was provided by Nix (2010). The bridge was originally designed using steel reinforcement; the use of GFRP reinforcing bars increased the overall capital cost of this bridge by 8%. However, further investigation into the per-year cost of the bridge deck is required due to the noncorrosive nature of the material and the extended design life the material provides.

The cost of the GFRP reinforced and steel reinforced concrete deck was \$59.25 /sq. feet and \$49.06/sq. feet respectively, a 21% increase. The Beaver Creek Bridge also had two additional girders to accommodate the GFRP deck, resulting in an additional cost of \$48,000.

When applied to the cost of the deck, the 2 extra girders resulted in an additional \$6.82/sq. feet, bringing the total cost of the GFRP reinforced deck to \$66.07/sq. feet. Altogether, the GFRP reinforced deck cost 35% more than the traditional steel reinforced deck. However, there is more to a bridge than just its initial cost. The design life of the Beaver Creek Bridge was 60 years compared to the 45 years of the RC steel bridge. The 60 year design life is a conservative estimate since there is little historical data for the performance of GFRP bars in bridges. The cost comparison on a per year basis is less dramatic, resulting in \$1.10/sq. feet /yr for the GFRP deck and \$1.09/sq. feet/yr for the steel deck, as shown in Table 8. The use of GFRP will also result in less scheduled maintenance and fewer resultant user delays.

Recent work investigating the durability of GFRP bars (Weber and Baquero 2010) recommends increasing the design life of GFRP decks to 100 years. This assumes no maintenance for the additional 40 years; therefore, the \$1.10/sq. feet /yr is spread over 100 years. Changing the design life to 100 years provides a per-year cost of \$0.66 /sq. feet/yr, as shown in Table 8 with a 40% reduction. The cost analysis for steel reinforcement with a 100 year design accounts for one deck replacement, as shown in Table 8. The extended design life of the GFRP reinforced deck provides a monetary advantage over traditional steel reinforced decks, despite its higher initial capital cost.

**Table 8. Deck Cost Analysis for Beaver Creek Bridge**

	GFRP Reinforced Deck		Steel Reinforced Deck	
	As Built	Extended Design life	As Built	Extended Design life
Deck Cost /sq. feet	\$59.25	\$59.25	\$49.06	\$115.12
Additional Girders	\$48,000	\$48,000	\$0	\$0
Girder Cost /sq. feet	\$6.82	\$6.82	\$0	\$0
Design Life (years)	60	100	45	100
Cost /sq. feet /yr	\$1.10	\$0.66	\$1.09	\$1.15

In a 100 year design life, the steel reinforced bridge deck will be replaced once.

Original Cost	\$49.06/ sq. feet
Replacement	\$49.06/ sq. feet
Traffic	\$7.00/ sq. feet
Demolition	\$5.00/ sq. feet
Disposal	\$5.00/ sq. feet
Total	\$115.12/ sq. feet

THIS PAGE LEFT INTENTIONALLY BLANK

## **5.0 CONCLUSIONS**

2 Glass Fiber Reinforced Polymer precast deck panels of the Beaver Creek Bridge on US-6 were monitored. The panels were monitored through every step of construction, from fabrication of the panels in the precast yard, through 3 lifts and transportation. The completed bridge at Beaver Creek underwent four truck load tests, and was monitored for over 2 years after opening to traffic. From the measurements and observations taken during this project, the following conclusions can be drawn:

1. To minimize shear stresses directly applied to the bars, the panels were lifted at 4 points using straps, supporting the panels from below. The maximum tensile strain in the GFRP bars was  $125 \mu\epsilon$ ; this strain corresponds to 0.8% of the ultimate strain. The strains observed during this project were consistent with those reported elsewhere (Benmokrane et al. 2006)
2. The deck panels were post-tensioned in the longitudinal direction of the bridge. The partial post-tensioning in the longitudinal direction caused a maximum compressive strain of  $164 \mu\epsilon$ , and an average strain of  $130 \mu\epsilon$ . From the initial jacking force of the post-tensioning strands, the theoretical change in strain of the concrete was calculated to be  $62 \mu\epsilon$ . This is approximately half the average strain of  $130 \mu\epsilon$  recorded by the VWSGs. However, the measured value includes other strain effects such as creep, shrinkage, and strand relaxation. Post-tensioning added to the continuity of the bridge deck and increased the shear transfer of the grouted keyways allowing the panels to transfer much of the shear load to adjacent panels.

3. The bridge underwent static and dynamic truck load tests, in which the west-bound lanes of the bridge were tested individually as well as simultaneously. During the static portion of the truck load test, the relative deflections between the bridge deck and the west diaphragm were measured. The maximum magnitude of the relative deflections was found to be 0.007 inches which is small and shows that there was good composite action between the deck panels, distributing the load from panel to panel. The test deflection of 0.007 inches was 93% less than the design deflection of 0.101 inches. However, the test loads were approximately 40% of the design loads and concrete compressive strength was 6,200 psi compared to a design strength of 4,000 psi. Furthermore, the deflections were 7% of the AASHTO limit of  $83/800 = 0.104$  inches. However, in subsequent monitoring from real traffic, relative deflections up to 0.15 inches were observed.
4. The live load deflections of the prestressed girders during the static truck load tests were found to be significantly smaller than the allowable deflection specified by the AASHTO Specifications (2009). The decreased girder spacing, and resultant increase in the number of girders, as well as the increased concrete compressive strength may account for this. For 2 trucks located at midspan weighing a total of 87.04 kips the maximum deflection observed was 0.13 inches. The small deflections observed across girders 1 -5, and the positive deflection observed in girder 6, provides evidence that panel-to-girder continuity was achieved via the blockouts.
5. GFRP panels were constructed and placed without damaging them in a way that would compromise their integrity and functionality in the long-term. There were no signs of cracking and the stresses and deflections were below the design limit. The maximum

calculated deflection while lifting was 0.34 inches and the maximum stress was 490 psi (tension).

6. The changes made to the design of the bridge to accommodate GFRP bars were successful in preventing the deck from cracking and maintained small service deflections.
7. The accelerations of the girders were measured at the midspan during the dynamic portion of the truck load test. A 43.2 kips truck traveling in the left hand lane at 65 mph demonstrated a vertical acceleration of 0.026g. The results from the other dynamic truck load tests were similar with respect to magnitude. The girder on which the maximum acceleration was recorded varied depending on the location of the truck. From the dynamic tests performed during this project, there is a small correlation between greater speed of the truck and greater maximum accelerations at midspan; however, the sample size was only 19 trucks. Given the nature of the accelerometer data, it is difficult to hypothesize on potential trends at this time regarding the correlation between weight of the truck and maximum acceleration; it has been shown that trucks weighing 40 kips to 80 kips give a maximum acceleration of 0.03 g to 0.06 g. There is not a significant trend in the sample data.
8. The damping ratio, dynamic displacements, period, frequency and impact factors were found from accelerometer data. From the first truck load test, the characteristics of the bridge are: a period of 0.12 sec; the damping ratio is calculated as 1.47% of critical damping; a maximum dynamic displacement of 0.014 inches from truck B during the September 2009 test over girder 4; and the impact factor is calculated as 1.18-1.20.
9. The cost of the GFRP reinforced deck was compared to the cost as if it were designed to be a traditional steel reinforced deck. The cost comparison on a per year basis was

determined to be \$1.10/sq. feet /yr for the GFRP reinforced deck and \$1.09/sq. feet /yr of the steel reinforced deck. Further investigation into the lifespan of GFRP reinforced decks was made and resulted in an increase in the design life and corresponding decrease in thy per year cost. Changing the design life to 100 years provides a per-year cost of \$0.66 /sq. feet/yr. The extended design life of the GFRP reinforced deck provided a monetary advantage over traditional steel reinforced decks, despite its higher initial capital cost.

10. Long term health monitoring is a successful way to track trends on strains, deflections and accelerations for performance history. Real time monitoring also provides the ability to capture snapshots of daily activity that can then be analyzed with respect to the traffic situation, i.e. construction, oversized loads, or other extreme events.

## **6.0 REFERENCES**

1. American Concrete Institute Committee 440, 2006, Guide for the Design and Construction of Structural Concrete Reinforced with FRP Bars (ACI 440.1R-06), American Concrete Institute, Farmington Hills, MI.
2. American Association of State and Highway Transportation Officials, 2009, AASHTO LRFD Bridge Design Guide Specifications for GFRP Reinforced Concrete Bridge Decks and Traffic Railings, 1st Edition, American Association of State Highway Transportation Officials, Washington, DC.
3. Benmokrane, B., El-Salakaway, E., Lackey, T., (2006). “Designing and testing of concrete bridge decks reinforced with glass FRP Bars”. Journal of Bridge Engineers, ASCE, 217-229.
4. Deitz, D. H., Harik I. E., and Gesund, H., (2003). “Physical Properties of Glass Fiber Reinforced Polymer Rebars in Compression”. Journal of Composites for Construction, ASCE. November 2003, No.363.
5. Nix, R., (October 2010). Personal Communication.
6. Tang, B.,(1997). “Fiber Reinforced Polymer Composites Applications in USA“, Department of Transportation-Federal Highway Administration, <<http://www.fhwa.dot.gov/bridge/frp/frp197.cfm> > (October 5 2010).
7. Weber, A., and Baquero, C. W., (2010). “New Durability Concept for FRP Reinforcing Bars”. Concrete International.
8. Liu, R. “Precast Concrete Bridge Deck Panels Reinforced with GFRP Bars”. Dissertation, University of Utah, Salt Lake City, Utah 2011.

9. Wong, K., and Hart, G.,(2000) *Structural Dynamics for Structural Engineers*, New York, New York
10. *SAP 2000*. Computer software. Vers. 14.2. Computers and Structures Inc. Web. 2011.

## LIST OF SYMBOLS AND ABBREVIATIONS

GFRP	=	Glass Fiber Reinforced Polymer
LVDT	=	Linear variable differential transformer
TLT	=	Truck load test
VWSG	=	Vibrating wire strain gauge
EP3	=	End panel three
P2-05	=	Phase two Panel five
ACI	=	American concrete institute
PCI	=	Precast Cast Institute
$E_c$	=	Modulus of elasticity of concrete
$I$	=	Gross moment of Inertia
$I_e$	=	Effective moment of Inertia
$\phi$	=	Curvature
$\varepsilon$	=	Strain
$d$	=	Distance between the top and bottom reinforcing mats
$M_t$	=	Theoretical moment
$M_{LL}$	=	Moment from Design Live Load
$l_{eff}$	=	Effective distance between girders
RC	=	Reinforced concrete